Phosphoproteomics after nitrate treatments reveal an important role for PIN2 phosphorylation in control of root system architecture.

Andrea Vega[1], Isabel Fredes[1], José O'Brien[1,2], Zhouxin Shen[3], Krisztina Ötvös[4,5], Eva Benkova[4], Steven P. Briggs[3] and Rodrigo A. Gutiérrez[1,*]

[1] Departamento de Genética Molecular y Microbiología, Pontificia Universidad Católica de Chile, Avda. Libertador Bernardo O'Higgins 340, Santiago, Chile. FONDAP Center for Genome Regulation. Millennium Institute for Integrative Biology (iBio), Santiago, Chile.

[2] Departamento de Fruticultura y Enología, Pontificia Universidad Católica de Chile, Avda. Vicuña Mackenna 4860, Santiago, Chile.

[3] Cell and Developmental Biology. University of California San Diego. San Diego, CA. United States of America.

[4] Institute of Science and Technology (IST) Austria, 3400 Klosterneuburg, Austria.

[5] Bioresources Unit, Center for Health & Bioresources, AIT Austrian Institute of Technology GmbH, 3430 Tulln, Austria.

* To whom correspondence should be addressed: rgutierrez@bio.puc.cl

Abstract

Nitrate is an important signaling molecule that commands genome-wide gene expression changes that impact metabolism, physiology, plant growth and development. Although gene expression responses to nitrate at the mRNA level have been characterized in great detail, the impact of nitrate signaling at the proteome level has been much less explored. Most signaling pathways involve post-translational modifications of key protein factors and chiefly among these modifications is protein phosphorylation. In an effort to identify new components involved in nitrate responses in plants, we performed analyses of the *Arabidopsis thaliana* root phosphoproteome in response to nitrate treatments via liquid chromatography coupled to tandem mass spectrometry. We identified 268 phosphoproteins that show significant changes at 5 min or 20 min after nitrate treatments. The large majority of these proteins (96%) are coded by genes that are not modulated at the expression level in response to nitrate treatments in publicly available transcriptome data. Proteins identified by 5 min include potential signaling-components such as kinases or transcription factors. In contrast, by 20 min, proteins identified were associated with protein binding, transporter activity or hormone metabolism functions. Interestingly, the phosphorylation profile of *NITRATE TRANSPORTER 1.1* (*NRT1.1)* mutant plants in response to nitrate at 5 min was significantly different (95%) as compared to wild-type plants. This result is consistent with the role of NRT1.1 as a key component of a nitrate signaling pathway that involves phosphoproteomic changes. Our integrative bioinformatics analysis highlights auxin transport as an important mechanism modulated by nitrate signaling at the post-translational level. We experimentally validated the role of PIN2 phosphorylation in both primary and lateral root growth responses to nitrate. Our data provide new insights into the phosphoproteome and identifies novel protein components that are regulated post-translationally, such as PIN2, in nitrate responses in *Arabidopsis thaliana* roots.

Introduction

Nitrogen (N) is the mineral nutrient required in the greatest amounts by plants. N is often scarce in natural and agricultural systems, constituting a major factor limiting plant growth and agricultural yield. During the last 50 years, global demand for synthetic N fertilizers has dramatically increased in response to growing agricultural demand. Depending on soil conditions and plant species, less than 50% of the applied N fertilizer is taken up by crops. Excess N may contaminate aquatic systems[1] or be released into the atmosphere as N-oxide gases[2,3], both leading to detrimental effects on the environment and human health.

The relevance of N for plants is exemplified by its effects on leaf growth[4], senescence[5], root system architecture[6,7], and flowering time[8,9]. Due to its importance, plants have evolved sophisticated mechanisms to adapt to fluctuating N availability. Furthermore, growth and developmental processes can be regulated by varying the amount of N supplied to plants. For instance, exogenous nitrate applications stimulate lateral root elongation, enabling root growth and colonization in nitrate-rich soil patches[10,11]. However, high nitrate concentrations reduce primary and lateral root elongation under homogeneous growth-conditions[12]. Nitrate is the main form of inorganic N for plants in natural and agricultural soils[13,14]. Besides its nutritional role, nitrate acts as a signaling molecule that regulates several genes involved in a wide range of biological processes[15,16]. With advances in genomic technologies and system approaches, thousands of nitrate-responsive genes have been identified in *Arabidopsis thaliana* roots and shoots[17–24]. These N-response genes include nitrate transporters, nitrate reductase (NR) and nitrite reductase (NiR), putative transcription factors, and stress response genes, as well as genes whose products play roles in glycolysis, N metabolism, and hormone pathways. Moreover, nitrate elicits local and systemic signals to synchronize its availability with plant growth and development[25–29]. Although transcriptional responses activated by nitrate have been described in great detail, it is clear that regulation at the post-translational level is key for N-responses[30,31].

The role of protein phosphorylation in response to nitrate was initially identified in post-translational modifications in N metabolism. The activity of NR, the enzyme that catalyzes the first step of nitrate reduction, is modulated by protein phosphorylation and then inhibited by 14-3-3 protein interaction[32,33]. Studies in spinach leaves using ^{32}P labeling and kinase assays demonstrated that the regulation of NR by light/dark and photosynthetic activity involves protein

phosphorylation[34,35]. A subsequent study showed that a 14-3-3 family protein interacts with and inactivates phosphorylated NR in the presence of covalent ions [32,36]. Earlier experiments also indicated that changes in gene expression in response to nitrate treatments require kinase and phosphatase activities. In maize leaves for example, treatments with inhibitors of calmodulin-dependent protein kinases repress nitrate induction of genes encoding nitrate assimilatory enzymes such as NR, NiR, glutamine synthetase 2 (GS2) and ferredoxin glutamate synthase (Fd-GOGAT)[37]. Conversely, inhibition of protein phosphatases blocked the nitrate-response of NR, NIR and GS2[37]. In another study, pharmacological inhibitors of serine-threonine protein phosphatase and tyrosine protein kinases repressed the nitrate-induced accumulation of transcripts for NR and NiR in barley leaves[38]. These early experiments suggested that changes in the status of protein phosphorylation were important for the regulation of gene expression in response to nitrate treatments.

The discovery that a kinase protein complex can directly phosphorylate the nitrate transceptor NRT1.1/NPF6.3 demonstrated that phosphorylation plays an important role in nitrate signaling. Under low-nitrate conditions, NRT1.1/NPF6.3 is phosphorylated in a threonine residue (T101) by CIPK23-CBL9 complex (CIPK, CLB-interacting protein kinase; CBL, Calcineurin B-like protein), shifting into a high-affinity nitrate transporter[31,39]. In contrast, at high-nitrate levels, NRT1.1/NPF6.3 is dephosphorylated at T101 and turns into a low-affinity transporter. Experiments with a mutant mimicking the phosphorylated form of the transceptor showed the importance of this phosphorylation for the regulation of gene expression at low nitrate concentrations[39]. Phosphorylation of NRT1.1/NPF6.3 also appears to play a role in the modulation of auxin transport and repression of lateral root emergence under low-nitrate conditions[40,41]. Conversely, the dephosphorylated form of NRT1.1/NPF6.3 is critical for up-regulation of *NITRATE TRANSPORTER 2.1* (*NRT2.1*) gene expression in response to nitrate[39,40]. Bouguyon *et al.* (2015)[40] studied different mutant alleles of NRT1.1/NPF6.3 (T101D, T101A and P492L substitution), and proposed a different NRT1.1/NPF6.3-dependent signaling mechanism. The short-term induction of *NRT2.1* at high nitrate is negatively affected by T101D substitutions but not by P492L and T101A. Long-term regulation of *NRT2.1* transcripts at high nitrate and repression of lateral root emergence at low nitrate showed an opposite pattern, where signaling was suppressed by both T101A and P492L mutations but not affected by T101 substitution. Another kinase involved in signaling is CIPK8[42]. In *cipk8* mutants, the rapid induction of genes or

primary nitrate response was strongly reduced (40-65% of WT levels), particularly in the low-affinity phase[42]. Both CIPK8 and CIPK23 are rapidly induced by nitrate treatments and downregulated in the *chl1-5* and *chl1-9* mutants, respectively[39,42]. More recently, the calcium sensor CBL1 and the protein phosphatase 2C (ABA-insensitive) ABI2 were also identified as components of this signaling pathway, which regulates NRT1.1/NPF6.3 transport and sensing[43]. The calcium sensor CBL1 also interacts with CIPK23 and this complex was dephosphorylated by ABI2[43].

In higher plants, CBL/CIPK complexes sense and decode Ca^{2+} signals, triggering specific transduction pathways (reviewed by [44]). Recent studies have shown that Ca^{2+} plays a role in nitrate signaling transduction and is important for the primary nitrate response in *Arabidopsis* roots[45]. Calcium is a key secondary messenger that triggers changes in signaling pathways, including changes in phosphorylation levels[46,47]. More recently, results published by Liu et al. (2017)[30] have contributed to our understanding of the relationship between Ca^{2+} signaling and the first layer of transcriptional regulators. They used the luciferase (LUC) reporter gene NIR-LUC, which exhibits a physiological nitrate response in transgenic *Arabidopsis* plants, to identify three CPKs (CPK10, CPK30, and CPK32) that activated the NIR-LUC reporter in an effective and synergistic manner. Additionally, CPK10, CPK30, and CPK32 phosphorylated the transcription factor NIN-LIKE PROTEIN 7 (NLP7) in a Ca^{2+} dependent manner[30], suggesting that CPK-NLP signaling is a key regulator of primary nitrate responses[48]. All these studies provide evidence that NRT1.1/NPF6.3, calcium and phosphorylation of target proteins are key elements of a signaling pathway involved in the nitrate response.

Global-scale proteomic analysis performed in *Arabidopsis* seedlings, mostly shoot organs, showed that nitrogen starvation and resupply (nitrate or ammonium) modulates protein phosphorylation over a time course of 30 min[49]. In general, proteins such as receptor kinases and transcription factors change their phosphorylation levels after nitrogen resupply at 5-10 min (fast response). Proteins involved in protein synthesis and degradation, central and hormone metabolism showed changes in their phosphorylation level after 10 min (late response). Another study showed that nitrate deprivation affects both protein abundance and phosphorylation status[50]. Nitrate deprivation assays revealed that some proteins, mostly involved in transport, contain sites that are dephosphorylated early in the response [50].

In this study, we performed quantitative time-course analyses of the *Arabidopsis* root phosphoproteome in response to nitrate via liquid chromatography coupled to tandem mass spectrometry detection (HPLC-MS/MS). We chose to focus on root-phosphoproteomics profiling in response to nitrate for several reasons: (i) phosphoproteomics and proteomics studies describe phosphorylation levels as more dynamic and mainly independent of protein abundance[51–53], suggesting that many proteins are regulated by phosphorylation independent of their changes in protein abundance. (ii) Previous global studies of N treatment focused on the proteome and phosphoproteome in *Arabidopsis* seedlings, which interrogates mostly shoot tissues[49,50]. In order to search for new N-regulatory factors, our experimental approach focused on *Arabidopsis* roots because early sensing and responses to N-supply occur in the roots. Several studies have shown that HPLC-MS/MS provides accurate estimates of dynamic phosphorylation levels *in vivo*[54–57].

We used HPLC-MS/MS to identify phosphorylated proteins with differential profiles in response to nitrate treatments at 0, 5 or 20 min. We found that the nature of these phosphorylated proteins differed significantly from those encoded by genes implicated in nitrate via transcriptomic studies. We found different types of phosphoproteins changing at 5 or 20 min after nitrate treatments. Interestingly, the large majority of these changes depend on NRT1.1/NPF6.3. Kinases and transcription factors were over-represented at 5 min, while proteins involved in protein binding and transporter activity were common by 20 min of nitrate treatments. We found several phosphoproteins involved in auxin transport, including the auxin efflux-carriers PIN2 and PIN4. We validated the role of PIN2 and found dephosphorylation of PIN2 to be important for modulation of root system architecture in response to nitrate. Our analysis reveals that the nitrate signaling pathway mediated by NRT1.1/NPF6.3 leads to important changes in protein phosphorylation patterns and proposes new players that participate in the developmental responses to nitrate in plants.

Results

Phosphoproteome analysis of *Arabidopsis* roots in response to nitrate treatments.

In an effort to identify new components involved in nitrate responses in plants, we performed large-scale mass spectrometry-based phosphoproteome experiments following nitrate treatments in *Arabidopsis* roots. *A. thaliana (L.) Columbia-0* (Col-0) seedlings were grown hydroponically, with a full nutrient solution (Murashige and Skoog basal medium without N) containing 1 mM ammonium as the only N source for 14 days (time 0, see experimental procedures). Two-week-old plants were treated with 5 mM KNO_3 or KCl, as control. We and other laboratories have used this experimental setup in prior studies because it elicits robust primary nitrate responses in *Arabidopsis* plants[7,16,45,58,59]. A label-free high-performance liquid chromatography-tandem mass spectrometry (HPLC-MS/MS) method was used to identify changes in protein phosphorylation at 0, 5 or 20 minutes after nitrate treatments. We chose these time points because they have shown to be effective in describing transient and persistent protein phosphorylation responses[49,55]. Moreover, this experimental design allows for comparison with transcriptomics data obtained using the same experimental conditions[7,45,58]. For phosphoproteome analysis, we used a previously validated experimental pipeline[52,53,60]. Briefly, phosphopeptides were enriched using cerium oxide affinity capture and analyzed with a HPLC-MS/MS instrument (Figure S1). The spectra were assigned to specific peptide sequences by the MASCOT search engine (FDR < 0.1%). We quantified the relative abundance of each phosphoprotein using average normalized spectral counts (SPCs) of the total number of spectral-peptide matches to protein sequences in three independent biological replicates for each treatment condition. In total, we identified and measured 6,560 unique phosphopeptides which unambiguously mapped to 2,048 phosphoprotein groups (Supplemental Table S1). The majority of identified phosphopeptides (82%) were phosphorylated in a single residue (Figure S2A). The relative distribution of each phosphorylated residue – 80% serine, 18% threonine, and 2% tyrosine (Figure S2B) – was consistent with prior plant phosphoproteomic studies[50,54,61]. The identified phosphopeptides were mapped and grouped in phosphoprotein groups, where proteins that shared peptides were clustered together. A group leader was assigned to each group, based on having the highest number of peptide identifications; throughout the remainder of the article, “phosphoproteins” is synonymous with “group leaders”. The majority of the identified phosphoproteins present one (50%), two (25%) or three (12%) phosphorylated peptides (Figure S2C) with similar distributions of

phosphorylated residue (69% Ser, 28% Thr and 3% Tyr; Figure S2D). We recognized phosphoproteins across several biological process, subcellular compartments and cellular functions based on the Gene Ontology (GO) classification (Figure S3). No overrepresented GO categories were observed when comparing against the *Arabidopsis* genome, showing that our experimental strategy was unbiased with regards to annotated protein functions, subcellular locations or biological processes and represents an unbiased *Arabidopsis* proteome sampling.

To identify nitrate-regulated phosphoproteins in *Arabidopsis* roots we performed statistical analysis using analysis of variance (significance: $p < 0.05$). We identified 268 phosphoproteins that were significantly altered under our experimental conditions. We found 62 phosphoproteins regulated at 5 min after nitrate treatments, 40 of which were induced (Figure 1A). We found 152 phosphoproteins differentially regulated at 20 min, 113 of which were induced by the nitrate treatments. The large majority of phosphoproteins were found to be nitrate-regulated at only one time-point, indicating that most changes in the phosphoproteome are transient with an early (5 min) and late (20 min) component in response to nitrate treatments. Two previous studies characterized the phosphoproteome in response to nitrate-depletion[49] or nitrate-resupply[50] (Figure 1C). Response to nitrate-resupply resulted in 10 common phosphoproteins and nitrate-deprivation in 6 common proteins. These proteins were mostly associated with nitrate metabolism, such as transporters (NRT2.1; ammonium transporter 1.3, AMT1.3), the *Arabidopsis* H^+-ATPase 2 (AHA2) proton pump, and nitrate reductase 2 (NIA2). The comparison of the phosphoproteins identified here with transcriptome data revealed that 96% of the phosphoproteins are encoded by genes that do not change expression at the mRNA level (Figure S4). We compared our results with an integrated analysis of available root microarray data under contrasting nitrate conditions (27 experimental datasets corresponding to 131 arrays[62]). This study identified a group of 2286 nitrate-responsive genes regulated at transcription levels. Only 11 of these genes were found in our phosphoproteomic dataset.

Our approach identified new genes coding for phosphoproteins putatively involved in nitrate responses. Changes in phosphorylation patterns improve our understanding of signaling mechanisms that connect nitrate transporters/sensors with transcriptomic response and other biological processes. The small overlap between the phosphoproteomic studies to date highlights the importance of ours and additional future studies to address this important aspect of posttranslational modifications in response to N-signals in plants.

Functional enrichment in the phosphoproteome reveals distinctive signaling and regulatory processes occurring in early and late responses to nitrate.

To evaluate the biological significance of the phosphoproteome patterns observed in response to nitrate, hierarchical clustering analysis was performed on the phosphoprotein dataset at 5 and 20 min following nitrate treatments in Col-0 roots (Figure 2). In order to identify the most prominent functional categories affected, we searched for overrepresented biological terms in each cluster using the BioMaps program[63] and the PANTHER classification system[64,65] (significance: $p < 0.05$, corrected by FDR). This analysis highlighted several signaling, regulatory or metabolic functions differentially associated with early (5 min) and late (20 min) components in response to nitrate treatments. "DNA binding" and "Nucleic acid binding" categories were overrepresented in cluster 6, containing phosphoproteins that increase their levels at 5 min and do not change at 20 min. This cluster also includes previously undescribed transcription factors (TFs) in the N-response cascade in diverse transcriptomic studies[21–24,66]. In contrast, cluster groups containing mostly phosphoproteins that changed their levels at 20 min in response to nitrate were enriched in the functional categories: "transport" and "nitrogen compounds metabolism" (clusters 2 and 8). Consistent with this, increases in phosphoprotein levels in response to nitrate were observed in NRT2.1, the lysine–histidine-like transporter 4 (LHT4), the UDP-Arabinofuranose Transporter 4, AMT1-3 and the K+-transporter 8 (KUP8) only at 20 min following nitrate treatment. Increased abundance of the phospho-peptide Ser-501, corresponding to NRT2.1, was observed at 20 min after nitrate treatment. This site is localized in a C-terminal phosphorylation hotspot (Phosphorylation site database and predictor Phosphat4.0[67,68]) and was also identified in nitrate-deprivation experiments with an opposite phosphorylation response[50]. Also, phosphopeptides for AMT1.3 with phosphorylation at Thr-464 and Ser-487 were identified as "up-regulated" by nitrate treatments at 20 min. The phosphorylation of both sites inhibits transport function[69] and were also identified as phosphopeptides in nitrate deprivation[50] and resupply[49] experiments. We also found that nitrate strongly increased levels of phosphorylated nitrate reductase NIA2 at the highly conserved and regulatory site Ser-534[70]. These results are consistent with previous studies and suggest overall regulation of N metabolism by phosphorylation of key players by 20 min after nitrate treatments.

The final group of clusters showed enrichment in signaling and regulatory pathways, with different profiles at 5 min and 20 min. Clusters 1, 5, and 7, contained phosphoproteins with opposite regulation at 5 and 20 min, and showed proteins related to microRNA processing, phosphoinositide and phosphatidylinositol binding functions. Phosphoinositides can act in signaling pathways and serve as precursors for phospholipase C (PLC)-mediated signaling. A previous study in our laboratory implicated a PLC-activity in the nitrate signaling pathway[45]. Our results are consistent with these results and show that PLC2, represented by the phosphopeptide Ser-280, was identified as up-regulated in response to nitrate at 20 min (in Cluster 1). Cluster 10 is interesting for nitrate responses because it includes many components involved in classical processes regulated by nitrate in *Arabidopsis* roots. For instance, auxin and lateral root development are biological functions enriched in this group, which is consistent with auxin pathways being modulated by nitrate[16,71]. Several reports indicate that auxin acts as regulator of root system architecture in response to nitrate availability[7,71,72].

Overall, our dataset captures the dynamic effects of N-signaling on phosphoproteome profiles, which implicate a cascade of nonoverlapping processes in early and late responses. The earliest steps in the N phospho-dynamics were involved in signal transduction and transcription factor activity. In contrast, the later phosphoprotein data-set was enriched in metabolic, transport and root developmental processes. These temporal mechanisms show a transition of phosphorylation dynamics from phosphoproteins essential to signaling networks to proteins associated with biological processes involved in nitrate response.

NRT1.1/AtNPF6.3 is essential for transient phosphoprotein changes in response to nitrate treatments

The only nitrate sensor described to date is the nitrate transporter, NRT1.1/NPF6.3[39,73]. In order to understand the importance of NRT1.1/NPF6.3 for nitrate elicited changes in the phosphoproteome observed, we analyzed the phosphoproteomic profile of roots treated with 5 mM KNO3 or KCl (control) in a *nrt1.1-null* background (mutant *chl1-5*), using the same experimental conditions described above. 74% of phosphoproteins were detected in both datasets, yet only 5% of the nitrate-phosphoproteome response observed in wild-type plants was maintained in the *chl1-5* mutant (Figure 3). Moreover, 95% of phosphoprotein levels were altered in the *chl1-5* mutant plants. This result indicates that this gene is important for modulating protein phosphorylation in

response to nitrate, in addition its established role as nitrate transceptor.

Our analysis indicates that NRT1.1/NPF6.3 is critical for maintaining the *Arabidopsis* phosphoproteome in response to nitrate availability. It also denotes that NRT1.1/NPF6.3 function is required for rapid changes in phosphorylation of key proteins in response to nitrate in *Arabidopsis* roots. For example, phosphorylated peptides that map to proteins associated with nitrogen metabolism (NRT2.1, AMT1-3 and NIA2) were identified in *chl1-5* mutant roots, but their levels were not affected in response to nitrate.

Network analysis reveals regulatory sub-networks connected to transcription factors and potential kinases in response to nitrate.

To uncover key biological processes modulated by changes in phosphorylation, we performed a multinetwork analysis with our phosphoproteomics data. We generated this network by integrating different levels of information, including protein-protein interactions from BioGRID[74], predicted protein-DNA interactions of *Arabidopsis* TFs (DapSeq)[75,76], *Arabidopsis* metabolic pathways (KEGG), and miRNA-RNA, as described previously[16]. We also integrated kinase-substrate predictions and identified the most significant phosphorylation motifs and their predicted kinase families from our phosphoproteomic datasets using the Motif-X algorithm[77] and the PhosPhAt Kinase-Target interactions database[78] (Figure S5). We used the Cytoscape[79] software to visualize the resulting network, wherein genes that encoded each phosphoprotein were represented as nodes linked by edges that signify any of the functional relationships annotated in the various databases indicated above. We generated a network of 206 nodes with 700 interactions (Figure 4A). Although the majority of these genes are not regulated by nitrate at the mRNA level, they form a highly interconnected network which includes potential regulatory transcription factors and kinase components. They are connected by multiple edges, including protein-protein, protein-DNA, and metabolic interactions. This result suggests that the products of these genes form connected biological modules that are coordinately regulated at the post-translational level. This network included several TFs with a high number of regulatory links. The most connected were the Trihelix transcription factor 1 (GTL1), the WRKY DNA-binding protein 65 (WRKY65), and the RELATED TO VERNALIZATION 1 (RTV1) transcription factors, which had not previously been characterized in the context of nitrate response. Intriguingly, GTL1 regulates root hair growth in *Arabidopsis*[80], which has recently been described as a biological process modulated

by nitrate treatments under the same experimental conditions[81]. A previous study indicated that WRKY65 interacts at the protein level with the mitogen-activated protein kinase 10 (MPK10), which binds with the lateral organ boundaries domain 16 (LBD16), LBD18, and LBD29 transcription factors[82,83]. These LBDs are inducible by auxin and play a role in the formation of lateral roots[83]. In addition, MPK10 interacted with other genes involved in the auxin response[82], while LBD29 regulated genes involved in auxin transport, including auxin efflux-carriers PIN1 and PIN2[83]. This evidence suggests that WRKY65 could be involved in nitrate–auxin signaling crosstalk. These three TFs appear to coordinate different subnetworks largely involved in auxin transport and nitrogen metabolism. Consistent with this observation, analysis of over-represented gene ontology annotations highlights the importance of auxin transport (Figure 4B). Other over-represented biological functions in our network were mRNA binding and splicing, regulation of translation and kinase activity (Figure 4B).

Overall, this network analysis highlights a potential role of multiples TFs in linking the N signal and regulatory nitrate responses that show significant enrichment for key functions in signaling pathways and validates the important role auxin plays in the nitrate-response of root system architecture.

PIN2 is important for modulation of root system architecture in response to nitrate treatments

Auxin is a key phytohormone in plants, involved in growth and developmental responses. Several reports have shown that auxin mediates root developmental responses to nitrate availability[7,16,71,72,84–86]. Nitrate can regulate auxin biosynthesis, transport and accumulation. In response to nitrate, several auxin-related modules are regulated, including the upregulation of auxin receptor AUXIN SIGNALING F-BOX 3 (AFB3) and the feedback regulation by miR393[7,71]. This auxin-signaling component in response to nitrate is implicated in both primary and lateral root growth[7]. Other important evidence comes from the analyses of the *Arabidopsis* transcriptomic response upon nitrate treatments. They show that several genes involved in auxin transport are affected, including auxin efflux-carriers PIN1, PIN4 and PIN7[16,71]. Moreover, the nitrate transceptor NRT1.1/NPF6.3 not only senses and transports nitrate but can also transports auxin, a process that regulates auxin-localization patterns and lateral-root elongation[84]. Consistent with these prior observations, auxin transport was conspicuous throughout our entire phosphoproteomic

337 analysis (Figure 2 and 4). PIN phosphorylation has been shown to be essential for auxin transport
338 and distribution[87–92]. PINs phosphorylation in conserved serine and/or threonine of the central loop
339 controls intracellular trafficking, recycling and polar membrane localization of PIN proteins
340 (Review by[87]). Previous studies indicate that PIN polar localization explains auxin fluxes and
341 distribution patterns, which could mediate differential growth in diverse plant tissue such as
342 roots[91,93]. To validate the relevance of phosphorylation in auxin transport and its connection with
343 nitrate response, we chose the auxin efflux-carrier PIN2 (identified in our experimental dataset)
344 due to its potential role in linking nitrate and changes in root system architecture (RSA). We found
345 an uncharacterized PIN2 phosphorylation site (Ser439) at the end of the hydrophilic cytoplasmic
346 loop (C-loop, Figure 5A). Its phosphopeptide levels decreased by close to 75% in response to
347 nitrate treatments by 5 min (Figure 5B). PIN2 belongs to the PIN-FORMED protein family of
348 auxin transporters and is the principal component mediating basipetal auxin transport in roots[94,95].
349 This polar auxin transport is essential for root gravitropism[95] and lateral root formation[96].
350 Intriguingly, we detected only one phosphorylated peptide for PIN2 in response to nitrate. Protein
351 sequence alignment indicated that this phosphosite is highly conserved in different plant species
352 representing gymnosperm, mono- and dicotyledonous plant lineages of seed plants (Figure 5A).
353 This phosphopeptide has also been described as down-regulated after auxin treatment but its
354 function remains an open question[57].

355 As a first step to understand the function of PIN2 phosphorylation in the nitrate response,
356 we performed a Phos-tag Western Blot analysis to confirm the changes in PIN2 phosphorylation
357 after nitrate treatment. We detected two, fast- and slow-mobility, PIN2 specific bands indicating
358 the presence of two phospho-populations in response to nitrate: one more and another less
359 phosphorylated PIN2. In contrast, only one slow-mobility band corresponding to the more
360 phosphorylated PIN2 subpopulation could be observed at time 0 (ammonium-supplied roots) or
361 under control conditions (KCl-treated roots) (Figure 5C). To assess whether these changes in PIN2
362 phosphorylation status are a result of a change in protein abundance, we analyzed PIN2-GPF
363 protein levels by Western Blot under our experimental conditions. We introgressed the construct
364 *PIN2::PIN2-GFP* (*PIN2^{wt}-GFP*) into the *pin2* loss-of-function mutant plant *eir1-1*[97]. No
365 differences in protein levels were observed in roots treated with nitrate as compared to roots at
366 time 0 (Figure 5D). To understand the function of this specific PIN2 phosphosite Ser439, we also
367 analyzed the protein levels in *pin2* null mutant complemented with phospho-null

(*PIN2::PIN2^{S439A}-GFP*) or phospho-mimic (*PIN2::PIN2^{S439D}-GFP*) versions of PIN2-GFP. Similarly, PIN2 protein concentrations were similar when our experimental conditions mimicked PIN2 phospho-modifications (Figure 5D). Moreover, no regulation at the mRNA level was observed in *PIN2* during nitrate responses (Figure 5E). These results demonstrated that nitrate regulates PIN2 at the posttranslational level, causing de-phosphorylation of PIN2 at a specific phosphosite.

Next, we evaluated the role of PIN2 in root system architecture (RSA) in response to nitrate treatments. We grew wild-type (Col-0) and *pin2* mutant (*eir1.1)* plants for 2 weeks on ammonium as sole N source (time 0) and evaluated RSA after nitrate treatments. We measured primary root length 3 days after 5 mM KNO_3 or KCl treatments. As expected for this experimental set up, we found that nitrate-treated wild-type plants developed shorter primary roots as compared to KCl-treated plants, consistent with earlier results indicating that nitrate treatments inhibit primary root elongation under these experimental conditions[7] (Figure 6A). However, primary roots of *eir1-1* plants were not significantly inhibited by nitrate treatments as compared to wild-type plants. We also analyzed the density of lateral roots in response to nitrate treatments. In wild-type plants, nitrate treatments increased the number of lateral roots (emerged and initiating) as compared with KCl treatments (Figure 6B). In contrast, the lateral root response to nitrate treatment was altered in the *eir1-1* mutant and the density of lateral roots was significantly reduced as compared with wild-type plants (Figure 6B). These results show that PIN2 plays an important role in modulating RSA in response to nitrate treatments.

PIN2 de-phosphorylation of Ser439 plays a role in modulating the root system architecture in response to nitrate treatments.

To understand the function of the PIN2 phosphosite identified in this study, we analyzed the *pin2* null mutant *eir1-1* complemented with phospho-null (S439A) or phospho-mimic (S439D) versions of PIN2-GFP. As PIN2 plays an important role in root gravitropism, we evaluated the gravitropic curvature in wild-type, *eir1-1* mutant plants and PIN2-GFP transgenic plants. All seedlings were germinated and grown in MS media in the absence of nitrate for 7 days, and then they were transferred to agar plates with or without nitrate. Agar plates were rotated 90° and root curvature was measured at 24 hours. As expected, *pin2* mutant plants showed an agravitropic

phenotype. Both *PIN2*^{S439D}*-GFP* and *PIN2*^{S439A}*-GFP* were able to rescue the agravitropic phenotype of *eir1-1* mutant plants. This result indicates that the phosphorylation status of PIN2 at S439 is not relevant for root gravitropic responses in *Arabidopsis* (Figure S6). This result also indicates that phosphorylation at S439 does not impair all PIN2 functions.

Next, we evaluated the RSA in response to nitrate treatments in the same phospho-mimicking (*PIN2*^{S439D}*-GFP*) or -null (*PIN2*^{S439A}*-GFP*) genotypes and compared it to wild-type plants. Plants were grown for 2 weeks on ammonium as sole N source and then treated with 5 mM KNO_3 or KCl for three days. Complementation of the *eir1-1* mutant with a wild-type version of PIN2 (*PIN2*^{wt}) restored normal RSA responses to nitrate (Figure 7). *eir1-1* mutant plants complemented with *PIN2*^{S439A} showed RSA changes similar to wild-type plants in response to nitrate treatments, albeit slightly less pronounced. Three days after nitrate treatments, primary root growth was inhibited 42% by nitrate in the *PIN2*^{S439A}*-GFP* genotype as compared with nitrate-treated wild-type plants (Figure 7A). Similarly, lateral root density in *PIN2*^{S439A}*-GFP* plants increased 47% as compared to wild-type plants in response to nitrate treatments (Figure 7B). In contrast at the end of the 3-day treatment, the primary root length and lateral root density did not differ between nitrate or KCl treatment in *eir1-1* mutant plants complemented with *PIN2*^{S439D}*-GFP*. This result, comparable to the response in *eir1-1* roots, indicates that regulation of PIN2 phosphorylation status at S439 is necessary for normal RSA modulation in response to nitrate treatments.

PIN2 phosphosite regulates polar plasma membrane localization in response to nitrate.

To explore the impact of nitrate-regulated phosphorylation of PIN2 on cellular localization, we examined the subcellular localization pattern in PIN2-GFP genotypes with phosphosite substitutions. PIN2^{WT}-GFP proteins were accumulated at the plasma membrane of epidermal and cortical cells, as previously described (Figure 8A)[86]. PIN2^{WT}-GFP fluorescence signal increased in epidermal and cortical cells 2 hours after nitrate treatments as compared to roots in control conditions (roots without nitrate treatments, Figure 8A). Interestingly, mutations at S439 altered this pattern. PIN2^{S439A}-GFP plants showed higher fluorescence in the plasma membrane even without nitrate treatment as compared to PIN2^{wt}-GFP or PIN2^{S439D}-GFP (Figure 8A). The total fluorescence in all experimental conditions analyzed here was similar (Figure 8B). In response to

nitrate, PIN2^{WT}-GFP and PIN2^{S439A}-GFP were accumulated at the plasma membrane of epidermal and cortical cells at comparable levels (Figure 8C and 8D). On the contrary, PIN2^{S439D}-GFP plants showed lower levels at epidermal and cortical cells in response to nitrate treatments as compared to PIN2^{WT}-GFP or PIN2^{S439A}-GFP (Figure 8C and 8D).

These results indicate that PIN2 phosphorylation status at S439 is important for a correct subcellular localization-pattern in response to nitrate treatments. Moreover, these results indicate that post-translational control impinging upon PIN2 localization is required for RSA changes in response to nitrate treatments.

Discussion

A key plant nutrient, N also acts as a signal that regulates a myriad of plant growth and developmental processes. Nitrate, a main N-source in natural and agriculture soils, elicits genome-wide changes in gene expression for thousands of genes involved in various biological functions. Nitrate responses have been characterized in great detail at the transcriptome level. However, post-translational modifications have not been characterized in detail. In this study, we evaluated phosphoproteomic profiles in *Arabidopsis* roots in response to nitrate treatments. We focused on characterizing early nitrate-elicited changes in protein phosphorylation. Protein phosphorylation and dephosphorylation plays a central role in modulating protein function in plant signaling-pathways involved in a wide range of processes relating to hormones, nutrients, and responses to stress [54–57,61,98].

Our analysis demonstrated that early and late changes in phosphoprotein levels occur in response to nitrate in roots. Furthermore, we identified candidates for nitrate-signaling and biological functions underlying the nitrate response in roots. Interestingly, the majority of proteins and corresponding genes identified in our analysis have not been previously associated with nitrate responses. The phosphoproteomic profile was characteristic of each time-point, showing dynamic changes in phosphorylation patterns in response to nitrate treatments. Early changes in phosphorylation levels (5 min) mainly affected proteins associated with gene regulation, including transcription factors and splicing process. These results are consistent with rapid and dynamic N-responses observed at the mRNA level described in previous studies[21–23,71]. Recent studies have identified new transcription factors[21–23] involved in the control of gene expression by nitrate. Interestingly, the majority of the transcription factors that we detected as differentially phosphorylated had not been identified as part of the nitrate response. The phosphoproteomic response to nitrate at 20 min revealed a group of different phosphoproteins, mostly involved in protein binding and transport. In this dataset, we found proteins known to be involved in nitrogen response as differentially phosphorylated, including the high-affinity nitrate transporter NRT2.1[49,50] and AMT1.3[69]. In our experimental conditions, site T464 in AMT1.3 was phosphorylated. Since phosphorylation of this site inhibits ammonium transport[69], the increased phosphorylation status at this site may be related to the fact that our experimental conditions focused on nitrate transport in *Arabidopsis* roots. We also identified phosphoproteins associated with signaling pathways and transcription factors, uncovering regulatory networks linked to

468 transcriptomic changes occurring later in the response to nitrate. The corresponding genes have
469 not been characterized in the context of nitrate responses. For instance, one potentially novel
470 regulatory factor is ABA-responsive element binding protein 3 (AREB 3), whose phosphoprotein
471 levels are increased in response to nitrate treatments. This transcription factor is involved in ABA
472 signaling[99,100]. Nitrate triggers ABA accumulation at the root tip[101] and several studies indicate
473 that ABA plays a role in regulation of lateral root growth by nitrate[102].

474 NRT1.1/NPF6.3 is the main nitrate sensor described to date[31,39]. Interestingly, we observed
475 important differences in the phosphoproteome of *chl1-5* mutant as compared to wild-type plants
476 in response to nitrate treatments. These results emphasize that NRT1.1/NPF6.3, calcium and
477 kinases/phosphatases make-up the canonical nitrate-signaling pathway of *Arabidopsis* roots.
478 Recent evidence showed that NRT1.1/NPF6.3 and PLC activity are required for nitrate-induced
479 increases in cytoplasmic Ca2+ levels[45]. Our results indicated that PLC2 phosphoprotein levels
480 increased in response to nitrate. Nitrate signaling pathways also involve CBL–CIPK complex and
481 CPK–NLP regulatory network (reviewed by [48]).

482 The transcriptomic nitrate-response was not mirrored at phosphoproteomic levels. This
483 lack of correlation between mRNA and protein or phosphoprotein levels has been documented in
484 other nitrogen-phosphoproteomic studies[49,50], plant responses to different stimulus[52,53] and other
485 organisms[103]. Furthermore, post-translational regulation does not require a change in gene
486 expression or *de novo* protein synthesis. Post-translational control is faster, allowing rapid
487 adaptation to environmental changes. Interestingly, the genes coding for nitrate-modulated
488 phosphoproteins identified in this study are highly co-expressed across many different
489 experimental conditions but not regulated by nitrate treatments[104]. This finding suggests that this
490 group of genes is functionally related and regulated at the mRNA level in response to several
491 endogenous or exogenous cues. In the context of nitrate responses, the products of these genes are
492 regulated at the post-translational level, uncovering a new layer of control that enables signal
493 crosstalk and fine tuning. Our results highlight the need for integrated analysis and data sets at
494 different levels to decipher plant responses to environmental cues.

495 It is now clear that auxin plays a central role in the plant root response to changes in nitrate
496 availability. Nitrate regulates primary root growth, lateral root initiation and elongation. Auxin in
497 turn is key during root development[96], particularly in initiation and growth of lateral roots[93].

Several reports show that auxin signaling, biosynthesis, transport, and accumulation are affected during nitrate responses[72,84], and transcriptomic analyses demonstrate that genes involved in auxin response are controlled by nitrate[7,16,71]. The main nitrate transporter NRT1.1/NPF6.3 can also transport auxin[84,86]. A recent study also showed that NRT1.1/NPF6.3 negatively regulates the *TAR2* auxin-biosynthetic gene and the *LAX3* auxin-influx transport gene at low nitrate concentrations, repressing lateral root development[105]. These results suggest that an interplay between nitrate signaling and auxin transport occurs at different levels[106–108]. Consistent with these findings, we found that the molecular function "auxin transport" was overrepresented in our cluster and network analyses. We showed that dephosphorylation of PIN2 in a novel phosphosite is a part of a regulatory mechanism for RSA responses triggered by nitrate. The phosphorylation/dephosphorylation of PIN proteins at specific sites (serine or threonine) located in their higher loops has been shown to play important roles in modulating PIN functions[88,91,92,109], including trafficking[110]. We showed that phosphorylation/dephosphorylation of PIN2 at S439 is important for PIN2 plasma membrane localization in epidermal and cortical cells in response to nitrate. Previous studies have shown that changes in PIN2 membrane localization and polarity interfere with PIN2 function in auxin transport with an impact on RSA during alkaline stress[111] or low phosphate[112]. In addition, recent studies showed that kinase cascade modules 3′-PHOSPHOINOSITIDE-DEPENDENT PROTEIN KINASE 1 (PDK1)-D6 PROTEIN KINASEs (D6PK) and PDK1- AGC1 kinase PROTEIN KINASE ASSOCIATED WITH BRX (PAX) regulate auxin distribution through PIN phosphorylation[113,114]. The phosphorylation of PIN affects PIN-mediated auxin transport, which controls plant growth[113] and other developmental processes[114]. These results suggest that PIN phosphorylation is part of a regulatory switch that strictly controls the directional transport of auxin and subsequent growth or developmental processes.

Our results suggest a model (Figure 9) in which nitrate promotes dephosphorylation of PIN2, which then impacts localization and auxin transport. Modulation of PIN2 function could affect growth of primary and lateral roots for optimal nutrient uptake. Beyond this new regulatory mechanism involving PIN2 protein, our phosphoproteomics results identify novel proteins, which may be interesting targets for future studies or biotechnological developments for improved nitrogen use-efficiency or crop yield.

Acknowledgements

This work was supported by Millennium Institute for Integrative Biology—iBio (Iniciativa Científica Milenio-MINECON), Fondo de Desarrollo de Areas Prioritarias (FONDAP) Center for Genome Regulation (15090007), Fondo Nacional de Desarrollo Científico y Tecnológico (FONDECYT) 1141097 (to RAG) and 1171631 (to AV). We would like to thank Unidad de Microscopía Avanzada UC (UMA UC).

Methods

Plant material and growth conditions.

Arabidopsis thaliana (L.) Heynh. Columbia-0 accession plants were used as wild type genotype in all experiments. The transgenic lines *PIN2::PIN2^{wt}-GFP, PIN2::PIN2^{S439D}-GFP* and *PIN2::PIN2^{S439A}-GFP* were introduced into *eir1-1* background (*pin2* null mutant plants), using strategies described previously. PIN2 lines were generated by Gybson assembly as described[115] using pGREEN backbone vector[116]. *PIN2::PIN2^{wt}-GFP* line was generated by insertion of *mGFP5* into *PIN2* coding sequence at nucleotide 1215 from ATG (between Thr405 and Arg406)[94,117]. For PIN2 promoter, 2178 bp upstream of the start codon was used. For the generations of *PIN2::PIN2^{S439D}-GFP* and *PIN2::PIN2^{S439A}-GFP* lines Serine 439 was replaced by aspartate (*PIN2^{S439D}*) or alanine (*PIN2^{S439A}*) by site-directed mutagenesis using Gibson Assembly.

Seeds were sterilized using 50% chlorine solution for 7 minutes and washed with sterile distilled water three times. Then, 1,500 *Arabidopsis* seedlings were placed into a hydroponic system (Phytatrays) with MS-modified basal salt media without N (Phytotechnology Laboratories, M531) supplemented with 1 mM ammonium as the only N source. Plants were grown under long-day photoperiods (16h light/ 8h dark and a temperature of 22 °C) for 14 days using a plant growth incubator (Percival Scientific, Inc.). At day 15, plants were treated with 5 mM KNO3 or 5 mM KCl for different time periods as indicated, using a protocol described previously[7]. For the phenotypic study of root response to nitrate, plants were grown as described above and were treated with 5 mM KNO3 or 5 mM KCl for 3 days.

Root architecture analysis.

For root phenotyping, plants were scanned in plates using an Epson Perfection V700 Photo scanner, and root length were measured using Fiji (v1.52). Initiating and emerging lateral roots were analyzed using DIC optics on a Nikon Eclipse 80i microscope, as described[7]. The data were statistically analyzed in the Graph Pad Prism 5 Program.

Protein extraction, phosphopeptide enrichment and mass spectrometry analysis.

Proteins were isolated from 1 g of frozen tissue per sample in each experimental condition (2-3 biological replicates). Sample preparation and protein extraction were performed using previously described methods[52,53]. Phosphopeptide enrichment was performed using 1% (w/v) colloidal CeO_2 into an acidified peptide solution at 1:10 (w/w). Mass spectrometry (MS) and peptide identification were based on protocols described previously[60]. Briefly, the generated spectra were analyzed on LTQ Velos linear ion trap tandem mass spectrometer (Thermo Electron) and phosphorylation sites were identified into a specific amino acid within a peptide by using the variable modification localization score in Agilent Spectrum Mill software[118]. Proteins were grouped based on their shared, common phophopeptides using principles of parsimony to address redundancy in proteins. Proteins classified within the same group share the same subset of phosphopeptides. Phosphorotein levels were quantified using spectral counting, as described previously[52,53]. MS data were normalized using the total number of spectral counts (SPC) for each MS run. Expressed phosphoproteins were defined by at least one SPC, after the application of quality score cutoff in MS analysis, in minimum two of the tree biological replicates. To identify nitrate-regulated phosphoproteins in *Arabidopsis* roots, raw data were log transformed and quantile normalized using R studio (https://rstudio.com) and MEV (http://mev.tm4.org/) software. The statistical multifactor analysis of variance (significance: $p < 0.05$) and *pos-hoc* analysis (significance: $p < 0.1$) were performed using R-studio. Encoded genes for phosphoproteins showing a similar pattern were analyzed and visualized using the average-linkage hierarchical clustering performed in Cluster 2.11 software, as described[119].

Gene network analysis

Arabidopsis encoded genes from our phosphoproteomics data were used. The gene network was generated by integrating different information, including protein-protein interactions from BioGRID[74], predicted protein-DNA interactions of *Arabidopsis* TFs (DapSeq)[75,76], *Arabidopsis* metabolic pathways (KEGG), and miRNA-RNA, as described previously[16]. This analysis also included predicted regulatory connections between phosphoproteins that we detected and kinase families. A kinase-substrate analysis, identifying the most significant phosphorylation motifs and their predicted kinases were performed using the Motif-X algorithm[77] and PhosPhAt Kinase-Target interactions database[78,120]. The resulting network was visualized using CYTOSCAPE software[79]. Cluster and Gene Ontology analysis into the network were achieved with ClusterMaker[121] and Bingo[121] tools for biological networks in cytoscape, respectively.

Phos-Tag PAGE and western immunoblotting

Affinity-based SDS PAGE identification of phosphorylated PIN2 isoforms were performed based on the protocols by Komis et al.[122] and the protocol given by the Phos-tag manufacturer (FUJIFILM Waco Chemicals) with slight modifications. *Arabidopsis* seedlings were grown on modified MS plates with ammonium as the only N source for 7 days. Next, seedlings ($n \geq 40$) were transferred to 5 mM nitrate amended agar plates and were incubated for 6 hours in light. Root samples were collected and homogenized in liquid N2 and then extracted with extraction buffer – 50 mM Tris-HCl, pH 7.5, 150 mM NaCl, 0.5% Triton X-100, 10 µM MG-132 and 0.1 mM PMSF - supplemented with protease and phosphatase inhibitor cocktails (Roche). Buffer volumes were adjusted to fresh weight (100 µL/100 mg tissues). Homogenized samples were centrifuged (4ºC, 15 min, 14000 rpm) and the supernatant was aliquoted (50µg protein/20-25 µL) and incubated at 45°C for 5 min in the presence of SDS loading buffer. Next, samples were loaded onto an acrylamide, Bis-Tris/HCl gel containing 50 µmol/L Phos-tagTM (AAL-107) pendant and Zn^{2+} as cation. Electrophoresis were run at 15 mA/gel for 5~ 6 hours or until the proteins are nicely separated (usually until the 25 kDa prestained protein marker just exit the gel assembly). Next gels were incubated for 30 minutes in transfer buffer containing 10 mM EDTA and were blotted to PVDF membranes using Tris/Glycine transfer buffer (25 mM Tris, 192 mM Glycine, 5% methanol). After blocking with 5% milk in TBST, the membrane was probed with α-PIN2 antibody (1:1000) for 2 h (RT) followed by α-rabbit IgG-HRP (1:15000) (Amersham) for 1 h (RT). After treating the membrane with Supersignal West Femto western chemiluminescent HRP substrate (Thermo Fisher Scientific), luminescent signals were detected using a liquid nitrogen–cooled charge-coupled device camera (Biorad). Digital images were analyzed, and signals were quantified using the Fiji software.

Confocal microscopy and image analysis

eir1-1 mutants complemented with *PIN2::PIN2^{wt}-GFP, PIN2::PIN2^{S439A}-GFP, PIN2::PIN2^{S439D}-GFP* were grown in modified MS plates with 1 mM ammonium as the only N source. 2 week-old plants were treated with 5 mM nitrate or without treatment (control conditions) for 2 hours. Roots were stained with propidium iodide (PI) and mounted on a slice for microscopic analysis. Images were acquired with Zeiss LSM880 confocal microscope with Airyscan equipped with a 40×Plan-Apochromat water immersion objective. Fluorescence signals for GFP (excitation 488 nm, emission 507 nm) and PI (excitation 536 nm, emission 617 nm) were detected. Microscopy

For image quantification (PIN2-GFP fluorescence intensity measurements) maximum intensity projections of confocal pictures were used in epidermis and cortex cells. Images were handled and analyzed with Zeiss blue (v3.1) and Fiji (v1.52) software. The experiment was performed with 3 biological replicates and 3-4 roots per experimental conditions were analyzed in each replicate.

Figure Legends

Figure 1. Characterization of the phosphoproteome profile in *Arabidopsis* roots in response to nitrate. Venn diagrams show the overlap of transient (5 min) and more persistent (20 min) changes in phosphoprotein relative-abundance after 5 mM nitrate treatments compared with each control condition (5 mM KCl) in *Arabidopsis* roots. (A) Overlap of phosphoproteins that were "up-regulated" by nitrate at 5 min (dark yellow) and 20 min (light yellow) (B) Overlap of phosphoproteins that were "down-regulated" by nitrate at 5 min (blue) and 20 min (light blue). (C) Identification of common phosphoproteins with published phosphoproteome data-sets in response to nitrate-deprivation[50] or nitrate-resupply[49].

Figure 2. Functional analysis of the phosphoproteome profile reveals signaling and regulatory processes occurring in early and late response to nitrate. The Figure showed a hierarchical clustering of nitrate-phosphoproteins with differential abundance at 5- or 20-min in response to nitrate. Phosphoproteins were normalized by Z-score and clustered using the Euclidean distance method with average linkage. The resulting clusters are shown as a heat map, where vertical bars and numbers to the right of the map denote the group (composed of all terminal nodes in the hierarchical tree) of phosphoprotein (correlation > 0.9) with a selected profile in early (5-min) or late (20-min) nitrate-response. Functional Gene Ontology (GO) categories significantly enriched (hypergeometric test with FDR, $p < 0.05$) in each cluster are highlighted to the right of the group.

Figure 3. Characterization of the phosphoproteome profile in response to nitrate in roots of *Arabidopsis* (Col-0) or *chl1-5* mutant plants. Percentage of nitrate-phosphoproteome responses at 5 min in wild-type plants that were maintained in *chl1-5*-mutant plant roots.

Figure 4. Gene network of nitrate-modulated phosphoproteins. (A) A network for the phosphoproteins (encoded genes) and putative kinases family were represented as nodes with color and shapes assigned according to function (e.g., blue squares: metabolic encoded-genes, green triangle: transcription factors or grey hexagon: kinase families). Edges connecting nodes represent functional interactions: transcription factor/TARGET regulation or predicted kinase-substrate control. The size of the triangle or hexagon is proportional to the number of targets of the TF or putative kinase family, respectively. (B) Over-represented biological processes in the phosphoproteins gene-network in response to nitrate (hypergeometric test with FDR, $p < 0.05$). The network was analyzed using BINGO and ClueGO tools in Cytoscape software. Over-represented gene ontology terms are shown as a node connected by edges based on semantic relationships as defined in the ontology.

Figure 5. Nitrate regulates PIN2 phosphorylation levels. (A) Schematic representation of the phosphosite (Ser 439) identified in PIN2 in our study. PIN2 protein possesses three specific regions: a region with five transmembrane segments (residues 1–163), a central hydrophilic loop extending from residue 164 to 482 and a region with five additional transmembrane segments (residues 483-647). Protein alignment with PIN2 or PIN-like proteins from different species indicates conservation of the serine residue in eudicot, monocot, and gymnosperm species. The red arrow highlights the S439 in the central loop of PIN2 proteins in different plants. The size of each protein in amino acids and the percentage of identity against the *Arabidopsis* PIN2 are indicated. (B) Levels of PIN2 phosphopeptide in our experiments. Bars represent the mean plus standard error of replicates. The asterisk indicates statistically significant differences ($p < 0.05$). (C) Detection of phosphorylation PIN2 by Phos-tag Western blotting. *Arabidopsis* plants (Col-0) were growth in ammonium as only nitrogen source, and treated with 5 mM KNO_3 or 5mM KCl as control. Total protein from roots were analyzed in SDS PAGE using Phos-tag to detect changes in phosphorylation status. Immunoblotting was performed with PIN2 antibody. Total proteins isolated from *eir1.1* roots were used as a negative control. (D) Western blot against PIN2 protein comparing nitrate treated (KNO3) and control (0) condition in *Arabidopsis* roots for all genotypes (*eir1-1* mutant background was

688 complemented with PIN2::PIN2^{wt}-GFP (PIN2^{wt}), PIN2::PIN2^{S439D}-GFP (PIN2^{S439D} phospho-mimic point
689 mutation) or PIN2::PIN2^{S439A}-GFP (PIN2^{S439A}, phospho-null point mutation). (E) Time-course analysis of
690 PIN2 mRNA levels in response to nitrate treatments in *Arabidopsis* roots.
691
692
693 **Figure 6. PIN2 is essential for nitrate regulation of primary root growth and lateral root density.** (A)
694 Primary root length of Col-0 wild type plants or *eir1-1* mutant plants was measured using the ImageJ
695 program 3 days after 5 mM KNO_3 or KCl treatments. (B) Number of initiating and emerging lateral roots
696 of Col-0 or *eir1-1* mutant plants were counted using light microscopy 3 days after 5 mM KNO_3 or KCl
697 treatments. Bars represent mean plus standard error of replicate experiments. Asterisk indicates statistically
698 significant difference between means (** $p < 0.01$).
699
700 **Figure 7. PIN2 dephosphorylation at S439 is important for modulation of primary root growth and**
701 **lateral root density in response to nitrate treatments**. Four different genotypes were used in these
702 experiments: *Arabidopsis* Col-0, *eir1-1* mutant background complemented with PIN2::PIN2^{wt}-GFP
703 (PIN2^{wt}), PIN2::PIN2^{S439D}-GFP (PIN2^{S439D} phospho-mimic point mutation) or PIN2::PIN2^{S439A}-GFP
704 (PIN2^{S439A}, phospho-null point mutation). All genotypes were grown hydroponically as described in
705 Methods and treated with 5 mM nitrate or KCl (A) Primary root length of the different genotypes was
706 measured using the ImageJ program 3 days after 5 mM KNO3 or KCl treatments (B) Number of initiating
707 and emerging lateral roots for all genotypes were counted using light microscopy 3 days after 5 mM KNO3
708 or KCl treatments. Bars represent mean plus standard errors. Asterisk indicate statistically significant
709 difference between means (*$p < 0.05$, **$p < 0.01$).
710
711 **Figure 8. PIN2 phosphorylation at S439 is important for modulation of protein localization in**
712 **response to nitrate treatments.** Three different genotypes were used in these experiments. *eir1-1* mutant
713 background complemented with PIN2::PIN2^{wt}-GFP (PIN2^{wt}), PIN2::PIN2^{S439D}-GFP (PIN2^{S439D} phospho-
714 mimic point mutation) or PIN2::PIN2^{S439A}-GFP (PIN2^{S439A}, phospho-null point mutation). All genotypes
715 were grown hydroponically as described in Methods and treated with 5 mM nitrate for 2 hours. (A) Confocal
716 microscopy using Zeiss Airyscan microscope and Zeiss-blue3.1 software was used to visualize PIN2 in
717 *Arabidopsis* roots. "e" denotes epidermis and "c" cortex. Scale bar = 20 µm. Tuckey box plots show PIN2-
718 GFP fluorescence intensity quantification (number of roots analyzed per experimental conditions = 8-10;
719 arbitrary units, a.u.) at the total cell membrane in roots (B), and from epidermal (C) and cortex (D) plasma
720 membrane in the different genotypes. Letters denote statistically significant difference between means as
721 determined by ANOVA analysis ($p < 0.05$).
722
723 **Figure 9. Schematic model of the role of PIN2 and phosphorylation in root nitrate responses.** Nitrate
724 treatments increase cytosolic calcium levels which interact with calcium binding proteins such as kinases
725 in the nitrate signaling pathway. Kinases phosphorylate protein targets such as transcription factors that can
726 mediate changes in gene expression in response to nitrate treatments. Nitrate can also cause
727 dephosphorylation of specific proteins. We showed nitrate treatments promote PIN2 dephosphorylation at
728 S439 which impact membrane localization and polarity of the PIN2 protein. This post-translational
729 regulatory mechanism is important for modulation of primary root growth and lateral root density in
730 response to nitrate treatments. Arrows and bar-headed solid lines represent activation or inhibition in
731 response to nitrate, respectively. Dashed arrows indicate proposed connections.
732
733
734
735

Figure S1. An overview of the root phosphoproteomic experiment. (A) Experimental design to identify changes in phosphoproteins in response to nitrate treatments in *Arabidopsis* thaliana roots. (B) Phosphoproteomic strategy for the enrichment, quantification and analysis of phosphopeptides.

Figure S2. An overview of the root phosphoproteomic analysis. (A) Distribution of the number of phosphosites per peptide for the indicated experimental data set (0, 5 or 20 minutes after nitrate treatment). (B) Relative distribution of phosphorylated residues in each peptide for indicated experimental data set. (C) Distribution of the number of phospho-peptides per protein for indicated experimental data set. (D) Percentage of phospho-proteins that present each phosphorylated residues for indicated data set.

Figure S3. Distribution of phosphoproteins across GO categories: biological process (A), cellular functions (B) and sub cellular compartment (C) for each experimental data set.

Figure S4. Comparison between phosphorproteomics and transcriptomic dataset in response to nitrate. The list of encoded genes in response to nitrate at transcriptomic (data-set 27 affymetrix experiment Canales et al., 2014) and phosphoproteomic (our work) levels were represented using the SUNGEAR tool (Poultney et al., 2007). The triangle shows each data set at the vertices: transcriptomic data-set, phosphoproteomic data (5 min), phosphoproteomic data (20 min).The size of the circles inside the figure are proportional with the number of genes in each data set, as indicated by the arrows around the circle. The number of genes is indicated in each circle.

Figure S5. Motif-X analysis of nitrate-responsive phosphopeptides. Amino acid sequences from -5 to +5 residues (the phosphorylated residue was 0) were scanned with the Motif-X algorithm. Motif list of phosphopeptides that met the criteria for phosphoproteins up-regulated (A) and down-regulated (B) by nitrate at 5 min. Motif list of phosphopeptides that met the criteria for phosphoproteins up-regulated (C) and down-regulated (D) by nitrate at 20 min See table S1 for the complete set of nitrate-regulated phosphoproteins.

Figure S6. Phosphoprotein PIN2 (S439) in root gravitropic response. pin2 null mutant background (*eir1-1)* complemented with non-modified or wild type version of PIN2 ($PIN2^{wt}$), phospho-null (S439A) or phospho-mimic (S439D) versions of PIN2 ($PIN2^{S439A}$ or $PIN2^{S439D}$, respectively) were grown in MS agar plate supplemented with 0 mM (A) or 5 mM (B) nitrate. At day 7, plates were rotated 90° and root curvature was measured at 24 hours with imageJ software. The figure shown a histogram of root gravitropic response where the length of black bars indicates the relative frequency of plants with the corresponding classes of angle. The average (μ) plus standard deviation of seedlings scored per line is indicated below each circle. Asterisk indicate statistically significant difference between means (**$p < 0.01$).

References

1. Robertson, G. P. & Vitousek, P. M. Nitrogen in Agriculture: Balancing the Cost of an Essential Resource. *Environ Resour* **34**, 97 125 (2009).

2. Crutzen, P. J., Mosier, A. R., Smith, K. A. & Winiwarter, W. N2O release from agro-biofuel production negates global warming reduction by replacing fossil fuels. *Atmos Chem Phys* **8**, 389–395 (2008).

3. Davidson, E. A. The contribution of manure and fertilizer nitrogen to atmospheric nitrous oxide since 1860. *Nat Geosci* **2**, 659 662 (2009).

4. Wirén, N. von *et al.* Differential regulation of three functional ammonium transporter genes by nitrogen in root hairs and by light in leaves of tomato. *Plant J* **21**, 167 175 (2000).

5. Vanacker, H. *et al.* Roles for redox regulation in leaf senescence of pea plants grown on different sources of nitrogen nutrition. *J Exp Bot* **57**, 1735 1745 (2006).

6. Zhang, H. *et al.* Dual pathways for regulation of root branching by nitrate. *Proc National Acad Sci* **96**, 6529–34 (1999).

7. Vidal, E. A. *et al.* Nitrate-responsive miR393/AFB3 regulatory module controls root system architecture in Arabidopsis thaliana. *Proc National Acad Sci* **107**, 4477–4482 (2010).

8. Marín, I. C. *et al.* Nitrate regulates floral induction in Arabidopsis, acting independently of light, gibberellin and autonomous pathways. *Planta* **233**, 539 552 (2010).

9. Gras, D. *et al.* SMZ/SNZ and gibberellin signaling are required for nitrate-elicited delay of flowering time in Arabidopsis thaliana. *J Exp Bot* **69**, 619–631 (2018).

10. Zhang, H. & Forde, B. G. An Arabidopsis MADS box gene that controls nutrient-induced changes in root architecture. *Science* **279**, 407 409 (1998).

11. Gojon, A., Nacry, P. & Davidian, J.-C. Root uptake regulation: a central process for NPS homeostasis in plants. *Curr Opin Plant Biol* **12**, 328 338 (2009).

12. Zhang, H., Rong, H. & Pilbeam, D. Signalling mechanisms underlying the morphological responses of the root system to nitrogen in Arabidopsis thaliana. *J Exp Bot* **58**, 2329 2338 (2007).

13. Crawford, N. M. & Forde, B. G. Molecular and developmental biology of inorganic nitrogen nutrition. *Arabidopsis Book* **1**, e0011 (2002).

14. Gutiérrez, R. A. Systems biology for enhanced plant nitrogen nutrition. *Science* **336**, 1673 1675 (2012).

15. Vidal, E. A. & Gutiérrez, R. A. A systems view of nitrogen nutrient and metabolite responses in Arabidopsis. *Curr Opin Plant Biol* **11**, 521–529 (2008).

16. Gutiérrez, R. A. *et al.* Qualitative network models and genome-wide expression data define carbon/nitrogen-responsive molecular machines in Arabidopsis. *Genome Biol* **8**, R7 (2006).

808 17. Wang, R., Okamoto, M. & Xing, X. Microarray Analysis of the Nitrate Response in Arabidopsis Roots and
809 Shoots Reveals over 1 , 000 Rapidly Responding Genes and New Linkages to Glucose , Trehalose-6-Phosphate ,
810 Iron , and Sulfate Metabolism. *Plant Physiology* **132**, 556–567 (2003).

811 18. Scheible, W.-R. *et al.* Genome-wide reprogramming of primary and secondary metabolism, protein synthesis,
812 cellular growth processes, and the regulatory infrastructure of Arabidopsis in response to nitrogen. *Plant Physiol*
813 **136**, 2483 2499 (2004).

814 19. Wang, R. *et al.* Genomic analysis of the nitrate response using a nitrate reductase-null mutant of Arabidopsis.
815 *Plant Physiol* **136**, 2512 2522 (2004).

816 20. Gutiérrez, R. A. *et al.* Insights into the genomic nitrate response using genetics and the Sungear Software
817 System. *J Exp Bot* **58**, 2359 2367 (2007).

818 21. Gaudinier, A. *et al.* Transcriptional regulation of nitrogen-associated metabolism and growth. *Nature* **563**, 259–
819 264 (2018).

820 22. Varala, K. *et al.* Temporal transcriptional logic of dynamic regulatory networks underlying nitrogen signaling
821 and use in plants. *Proc National Acad Sci* **115**, 6494–6499 (2018).

822 23. Brooks, M. D. *et al.* Network Walking charts transcriptional dynamics of nitrogen signaling by integrating
823 validated and predicted genome-wide interactions. *Nat Commun* **10**, 1569 (2019).

824 24. Gutiérrez, R. A. *et al.* Systems approach identifies an organic nitrogen-responsive gene network that is regulated
825 by the master clock control gene CCA1. *Proc National Acad Sci* **105**, 4939 4944 (2008).

826 25. Ruffel, S., Poitout, A., Krouk, G., Coruzzi, G. M. & Lacombe, B. Long-distance nitrate signaling displays
827 cytokinin dependent and independent branches. *J Integr Plant Biol* **58**, 226–229 (2016).

828 26. Ruffel, S. *et al.* Nitrogen economics of root foraging: transitive closure of the nitrate-cytokinin relay and distinct
829 systemic signaling for N supply vs. demand. *Proc National Acad Sci* **108**, 18524 18529 (2011).

830 27. Poitout, A. *et al.* Responses to Systemic Nitrogen Signaling in Arabidopsis Roots Involve trans -Zeatin in
831 Shoots. *Plant Cell* **30**, 1243–1257 (2018).

832 28. Chen, X. *et al.* Shoot-to-Root Mobile Transcription Factor HY5 Coordinates Plant Carbon and Nitrogen
833 Acquisition. *Curr Biol* **26**, 640–646 (2016).

834 29. Ohkubo, Y., Tanaka, M., Tabata, R., Ogawa-Ohnishi, M. & Matsubayashi, Y. Shoot-to-root mobile polypeptides
835 involved in systemic regulation of nitrogen acquisition. *Nat Plants* **3**, 1–6 (2017).

836 30. Liu, K. *et al.* Discovery of nitrate–CPK–NLP signalling in central nutrient–growth networks. *Nature* **545**, 311
837 316 (2017).

838 31. Liu, K. & Tsay, Y.-F. Switching between the two action modes of the dual-affinity nitrate transporter CHL1 by
839 phosphorylation. *Embo J* **22**, 1005 1013 (2003).

840 32. Bachmann, M., Huber, J. L., Liao, P.-C., Gage, D. A. & Huber, S. C. The inhibitor protein of phosphorylated
841 nitrate reductase from spinach (Spinacia oleracea) leaves is a 14-3-3 protein. *Febs Lett* **387**, 127–131 (1996).

842 33. Kaiser, W. M. *et al.* Modulation of nitrate reductase: some new insights, an unusual case and a potentially
843 important side reaction. *J Exp Bot* **53**, 875–882 (2002).

844 34. Huber, J. L., Huber, S. C., Campbell, W. H. & Redinbaugh, M. G. Reversible light/dark modulation of spinach
845 leaf nitrate reductase activity involves protein phosphorylation. *Arch Biochem Biophys* **296**, 58–65 (1992).

846 35. MacKintosh, C. Regulation of spinach-leaf nitrate reductase by reversible phosphorylation. *Biochimica Et*
847 *Biophysica Acta Bba - Mol Cell Res* **1137**, 121–126 (1992).

848 36. Athwal, G. S. & Huber, S. C. Divalent cations and polyamines bind to loop 8 of 14-3-3 proteins, modulating
849 their interaction with phosphorylated nitrate reductase. *Plant J* **29**, 119–129 (2002).

850 37. Sakakibara, H., Kobayashi, K. & Deji, A. Partial characterization of the signaling pathway for the nitrate-
851 dependent expression of genes for nitrogen-assimilatory enzymes using detached maize leaves. *Plant and Cell …*
852 (1997).

853 38. Sueyoshi, K. *et al.* Effects of inhibitors for signaling components on the expression of the genes for nitrate
854 reductase and nitrite reductase in excised barley leaves. *Soil Sci Plant Nutr* **45**, 1015 1019 (1999).

855 39. Ho, C.-H., Lin, S.-H., Hu, H.-C. & Tsay, Y.-F. CHL1 functions as a nitrate sensor in plants. *Cell* **138**, 1184 1194
856 (2009).

857 40. Bouguyon, E. *et al.* Multiple mechanisms of nitrate sensing by Arabidopsis nitrate transceptor NRT1.1. *Nat*
858 *Plants* **1**, 15015 (2015).

859 41. Bouguyon, E. *et al.* Nitrate Controls Root Development through Post-Transcriptional Regulation of the
860 NRT1.1/NPF6.3 transporter/sensor. *Plant Physiol* **172**, pp.01047.2016 12 (2016).

861 42. Hu, H.-C., Wang, Y.-Y. & Tsay, Y.-F. AtCIPK8, a CBL-interacting protein kinase, regulates the low-affinity
862 phase of the primary nitrate response. *Plant J* **57**, 264 278 (2009).

863 43. Léran, S. *et al.* Nitrate sensing and uptake in Arabidopsis are enhanced by ABI2, a phosphatase inactivated by
864 the stress hormone abscisic acid. *Sci Signal* **8**, ra43–ra43 (2015).

865 44. Kudla, J., Batistic, O. & Hashimoto, K. Calcium signals: the lead currency of plant information processing.
866 *Plant Cell Online* **22**, 541–63 (2010).

867 45. Riveras, E. *et al.* The Calcium Ion Is a Second Messenger in the Nitrate Signaling Pathway of Arabidopsis. *Plant*
868 *Physiol* **169**, 1397 1404 (2015).

869 46. Dodds, P. N. & Rathjen, J. P. Plant immunity: towards an integrated view of plant-pathogen interactions. *Nat*
870 *Rev Genet* **11**, 539 548 (2010).

871 47. Hashimoto, K. & Kudla, J. Calcium decoding mechanisms in plants. *Biochimie* **93**, 2054 2059 (2011).

872 48. Liu, K.-H., Diener, A., Lin, Z., Liu, C. & Sheen, J. Primary nitrate responses mediated by calcium signalling and
873 diverse protein phosphorylation. *J Exp Bot* (2020) doi:10.1093/jxb/eraa047.

874 49. Engelsberger, W. R. & Schulze, W. X. Nitrate and ammonium lead to distinct global dynamic phosphorylation
875 patterns when resupplied to nitrogen-starved Arabidopsis seedlings. *Plant J* **69**, 978 995 (2012).

876 50. Menz, J., Li, Z., Schulze, W. X. & Ludewig, U. Early nitrogen-deprivation responses in Arabidopsis roots reveal
877 distinct differences on transcriptome and (phospho-) proteome levels between nitrate and ammonium nutrition.
878 *Plant J* **88**, 717 734 (2016).

879 51. Huttlin, E. L. *et al.* A tissue-specific atlas of mouse protein phosphorylation and expression. *Cell* **143**, 1174 1189
880 (2010).

881 52. Walley, J. W. *et al.* Integration of omic networks in a developmental atlas of maize. *Science* **353**, 814 818
882 (2016).

883 53. Walley, J. W. *et al.* Reconstruction of protein networks from an atlas of maize seed proteotypes. *Proc National*
884 *Acad Sci* **110**, E4808 17 (2013).

885 54. Umezawa, T. *et al.* Genetics and phosphoproteomics reveal a protein phosphorylation network in the abscisic
886 acid signaling pathway in Arabidopsis thaliana. *Sci Signal* **6**, rs8 rs8 (2013).

887 55. Lin, L.-L. *et al.* Integrating Phosphoproteomics and Bioinformatics to Study Brassinosteroid-Regulated
888 Phosphorylation Dynamics in Arabidopsis. *Bmc Genomics* **16**, 1 17 (2015).

889 56. Zhang, M. *et al.* Phosphoproteome analysis reveals new drought response and defense mechanisms of seedling
890 leaves in bread wheat (Triticum aestivum L.). *J Proteomics* **109**, 290 308 (2014).

891 57. Zhang, H. *et al.* Quantitative phosphoproteomics after auxin-stimulated lateral root induction identifies an SNX1
892 protein phosphorylation site required for growth. *Mol Cell Proteomics* **12**, 1158 1169 (2013).

893 58. Alvarez, J. M. *et al.* Systems approach identifies TGA1 and TGA4 transcription factors as important regulatory
894 components of the nitrate response of Arabidopsis thaliana roots. *Plant J* **80**, 1 13 (2014).

895 59. Gifford, M. L., Dean, A., Gutiérrez, R. A., Coruzzi, G. M. & Birnbaum, K. D. Cell-specific nitrogen responses
896 mediate developmental plasticity. *Proc National Acad Sci* **105**, 803 808 (2008).

897 60. Facette, M. R., Shen, Z., Bjornsdottir, F. R., Briggs, S. P. & Smith, L. G. Parallel Proteomic and
898 Phosphoproteomic Analyses of Successive Stages of Maize Leaf Development. *Plant Cell* **25**, 2798 2812 (2013).

899 61. Lan, P., Li, W., Wen, T. N. & Schmidt, W. Quantitative Phosphoproteome Profiling of Iron-Deficient
900 Arabidopsis Roots. *Plant Physiol* **159**, 403 417 (2012).

901 62. Canales, J., Moyano, T. C., Villarroel, E. & Gutiérrez, R. A. Systems analysis of transcriptome data provides
902 new hypotheses about Arabidopsis root response to nitrate treatments. *Front Plant Sci* **5**, 22 (2014).

903 63. Katari, M. S. *et al.* VirtualPlant: a software platform to support systems biology research. *Plant Physiol* **152**, 500
904 515 (2010).

905 64. Mi, H., Muruganujan, A., Ebert, D., Huang, X. & Thomas, P. D. PANTHER version 14: more genomes, a new
906 PANTHER GO-slim and improvements in enrichment analysis tools. *Nucleic Acids Res* **47**, D419–D426 (2018).

907 65. Mi, H. *et al.* Protocol Update for large-scale genome and gene function analysis with the PANTHER
908 classification system (v.14.0). *Nat Protoc* **14**, 703–721 (2019).

909 66. Alvarez, J. M. *et al.* Transient genome-wide interactions of the master transcription factor NLP7 initiate a rapid
910 nitrogen-response cascade. *Nat Commun* **11**, 1157 (2020).

911 67. Heazlewood, J. L. *et al.* PhosPhAt: a database of phosphorylation sites in Arabidopsis thaliana and a plant-
912 specific phosphorylation site predictor. *Nucleic Acids Res* **36**, D1015–D1021 (2007).

913 68. Durek, P. *et al.* PhosPhAt: the Arabidopsis thaliana phosphorylation site database. An update. *Nucleic Acids Res*
914 **38**, D828–D834 (2010).

915 69. Lanquar, V. *et al.* Feedback inhibition of ammonium uptake by a phospho-dependent allosteric mechanism in
916 Arabidopsis. *Plant Cell Online* **21**, 3610 3622 (2009).

917 70. Su, W., Huber, S. C. & Crawford, N. M. Identification in vitro of a post-translational regulatory site in the hinge
918 1 region of Arabidopsis nitrate reductase. *Plant Cell* **8**, 519 527 (1996).

919 71. Vidal, E. A., Moyano, T. C., Riveras, E., Contreras-Lopez, O. & Gutierrez, R. A. Systems approaches map
920 regulatory networks downstream of the auxin receptor AFB3 in the nitrate response of Arabidopsis thaliana roots.
921 *Proc National Acad Sci* **110**, 12840–12845 (2013).

922 72. Ma, W. *et al.* Auxin biosynthetic gene TAR2 is involved in low nitrogen-mediated reprogramming of root
923 architecture in Arabidopsis. *Plant J* **78**, 70–79 (2014).

924 73. Wang, R., Xing, X., Wang, Y., Tran, A. & Crawford, N. M. A genetic screen for nitrate regulatory mutants
925 captures the nitrate transporter gene NRT1.1. *Plant Physiol* **151**, 472 478 (2009).

926 74. Oughtred, R. *et al.* The BioGRID interaction database: 2019 update. *Nucleic Acids Res* **47**, D529–D541 (2018).

927 75. Bartlett, A. *et al.* Mapping genome-wide transcription-factor binding sites using DAP-seq. *Nat Protoc* **12**, 1659–
928 1672 (2017).

929 76. Weirauch, M. T. *et al.* Determination and Inference of Eukaryotic Transcription Factor Sequence Specificity.
930 *Cell* **158**, 1431 1443 (2014).

931 77. Schwartz, D. & Gygi, S. P. An iterative statistical approach to the identification of protein phosphorylation
932 motifs from large-scale data sets. *Nat Biotechnol* **23**, 1391 1398 (2005).

933 78. Zulawski, M., Braginets, R. & Schulze, W. X. PhosPhAt goes kinases--searchable protein kinase target
934 information in the plant phosphorylation site database PhosPhAt. *Nucleic Acids Res* **41**, D1176-84 (2012).

935 79. Shannon, P. *et al.* Cytoscape: a software environment for integrated models of biomolecular interaction
936 networks. *Genome Research* **13**, 2498 2504 (2003).

937 80. Shibata, M. *et al.* GTL1 and DF1 regulate root hair growth through transcriptional repression of ROOT HAIR
938 DEFECTIVE 6-LIKE 4 in Arabidopsis. *Development* **145**, dev159707 (2018).

939 81. Canales, J., Contreras-López, O., Álvarez, J. M. & Gutiérrez, R. A. Nitrate induction of root hair density is
940 mediated by TGA1/TGA4 and CPC transcription factors in Arabidopsis thaliana. *Plant J* **92**, 305–316 (2017).

941 82. Popescu, S. C. *et al.* MAPK target networks in Arabidopsis thaliana revealed using functional protein
942 microarrays. *Gene Dev* **23**, 80–92 (2008).

943 83. Feng, Z., Zhu, J., Du, X. & Cui, X. Effects of three auxin-inducible LBD members on lateral root formation in
944 Arabidopsis thaliana. *Planta* **236**, 1227–1237 (2012).

945 84. Krouk, G. *et al.* Nitrate-Regulated Auxin Transport by NRT1.1 Defines a Mechanism for Nutrient Sensing in
946 Plants. *Dev Cell* **18**, 927 937 (2010).

947 85. Walch-Liu, P., Liu, L.-H., Remans, T., Tester, M. & Forde, B. G. Evidence that l -Glutamate Can Act as an
948 Exogenous Signal to Modulate Root Growth and Branching in Arabidopsis thaliana. *Plant Cell Physiol* **47**, 1045–
949 1057 (2006).

950 86. Mounier, E., PERVENT, M., Ljung, K., Gojon, A. & Nacry, P. Auxin-mediated nitrate signalling by NRT1.1
951 participates in the adaptive response of Arabidopsis root architecture to the spatial heterogeneity of nitrate
952 availability. *Plant Cell Environ* **37**, 162 174 (2013).

953 87. Barbosa, I. C. R., Hammes, U. Z. & Schwechheimer, C. Activation and Polarity Control of PIN-FORMED
954 Auxin Transporters by Phosphorylation. *Trends Plant Sci* **23**, 523–538 (2018).

955 88. Huang, F. *et al.* Phosphorylation of conserved PIN motifs directs Arabidopsis PIN1 polarity and auxin transport.
956 *Plant Cell Online* **22**, 1129 1142 (2010).

957 89. Zhang, J., Nodzynski, T., Pencík, A., Rolcík, J. & Friml, J. PIN phosphorylation is sufficient to mediate PIN
958 polarity and direct auxin transport. *Proc National Acad Sci* **107**, 918 922 (2010).

959 90. Friml, J. *et al.* A PINOID-Dependent Binary Switch in Apical-Basal PIN Polar Targeting Directs Auxin Efflux.
960 *Science* **306**, 862–865 (2004).

961 91. Weller, B. *et al.* Dynamic PIN-FORMED auxin efflux carrier phosphorylation at the plasma membrane controls
962 auxin efflux-dependent growth. *Proc National Acad Sci* **114**, 201614380–201614380 (2017).

963 92. Michniewicz, M. *et al.* Antagonistic Regulation of PIN Phosphorylation by PP2A and PINOID Directs Auxin
964 Flux. *Cell* **130**, 1044–1056 (2007).

965 93. Benková, E. *et al.* Local, Efflux-Dependent Auxin Gradients as a Common Module for Plant Organ Formation.
966 *Cell* **115**, 591–602 (2003).

967 94. Luschnig, C., Gaxiola, R. A., Grisafi, P. & Fink, G. R. EIR1, a root-specific protein involved in auxin transport,
968 is required for gravitropism in Arabidopsis thaliana. *Gene Dev* **12**, 2175–2187 (1998).

969 95. Müller, A. *et al.* AtPIN2 defines a locus of Arabidopsis for root gravitropism control. *Embo J* **17**, 6903 6911
970 (1998).

971 96. Laskowski, M. *et al.* Root system architecture from coupling cell shape to auxin transport. *Plos Biol* **6**, e307
972 (2008).

973 97. Roman, G., Lubarsky, B., Kieber, J. J., Rothenberg, M. & Ecker, J. R. Genetic analysis of ethylene signal
974 transduction in Arabidopsis thaliana: five novel mutant loci integrated into a stress response pathway. *Genetics* **139**,
975 1393 1409 (1995).

976 98. Vu, L. D. *et al.* Up-to-Date Workflow for Plant (Phospho)proteomics Identifies Differential Drought-Responsive
977 Phosphorylation Events in Maize Leaves. *J Proteome Res* **15**, 4304 4317 (2016).

978 99. Wang, P. *et al.* Quantitative phosphoproteomics identifies SnRK2 protein kinase substrates and reveals the
979 effectors of abscisic acid action. *Proc National Acad Sci* **110**, 11205–11210 (2013).

980 100. Kline, K. G., Barrett-Wilt, G. A. & Sussman, M. R. In planta changes in protein phosphorylation induced by
981 the plant hormone abscisic acid. *Proc National Acad Sci* **107**, 15986–15991 (2010).

982 101. Ondzighi-Assoume, C. A., Chakraborty, S. & Harris, J. M. Environmental Nitrate Stimulates Abscisic Acid
983 Accumulation in Arabidopsis Root Tips by Releasing It from Inactive Stores. *Plant Cell* **28**, 729–745 (2016).

984 102. Signora, L., Smet, I. D., Foyer, C. H. & Zhang, H. ABA plays a central role in mediating the regulatory effects
985 of nitrate on root branching in Arabidopsis. *Plant J* **28**, 655–662 (2001).

986 103. Vogel, C. & Marcotte, E. M. Insights into the regulation of protein abundance from proteomic and
987 transcriptomic analyses. *Nat Rev Genet* **13**, 227 (2012).

988 104. Obayashi, T. *et al.* ATTED-II in 2014: evaluation of gene coexpression in agriculturally important plants. *Plant*
989 *Cell Physiol* **55**, e6(1 7) (2014).

990 105. Maghiaoui, A. *et al.* The Arabidopsis NRT1.1 transceptor coordinately controls auxin biosynthesis and
991 transport to regulate root branching in response to nitrate. *J Exp Bot* (2020) doi:10.1093/jxb/eraa242.

992 106. Krouk, G. Hormones and nitrate: a two-way connection. *Plant Mol Biol* **91**, 599 606 (2016).

993 107. Krouk, G. *et al.* A framework integrating plant growth with hormones and nutrients. *Trends Plant Sci* **16**, 178
994 182 (2011).

995 108. Vega, A., O'Brien, J. A. & Gutiérrez, R. A. Nitrate and hormonal signaling crosstalk for plant growth and
996 development. *Curr Opin Plant Biol* **52**, 155–163 (2019).

997 109. Dhonukshe, P. *et al.* Plasma membrane-bound AGC3 kinases phosphorylate PIN auxin carriers at TPRXS(N/S)
998 motifs to direct apical PIN recycling. *Development* **137**, 3245 3255 (2010).

999 110. Ganguly, A., Park, M., Kesawat, M. S. & Cho, H.-T. Functional Analysis of the Hydrophilic Loop in
1000 Intracellular Trafficking of Arabidopsis PIN-FORMED Proteins. *Plant Cell* **26**, 1570–1585 (2014).

1001 111. Xu, W. *et al.* PIN2 is required for the adaptation of Arabidopsis roots to alkaline stress by modulating proton
1002 secretion. *J Exp Bot* **63**, 6105–6114 (2012).

1003 112. Kumar, M. *et al.* Arabidopsis response to low-phosphate conditions includes active changes in actin filaments
1004 and PIN2 polarization and is dependent on strigolactone signalling. *J Exp Bot* **66**, 1499–1510 (2015).

1005 113. Tan, S. *et al.* The lipid code-dependent phosphoswitch PDK1–D6PK activates PIN-mediated auxin efflux in
1006 Arabidopsis. *Nat Plants* 1–14 (2020) doi:10.1038/s41477-020-0648-9.

1007 114. Xiao, Y. & Offringa, R. PDK1 regulates auxin transport and Arabidopsis vascular development through AGC1
1008 kinase PAX. *Nat Plants* 1–12 (2020) doi:10.1038/s41477-020-0650-2.

1009 115. Gibson, D. G. *et al.* Enzymatic assembly of DNA molecules up to several hundred kilobases. *Nat Methods* **6**,
1010 343–345 (2009).

1011 116. Hellens, R. P., Edwards, E. A., Leyland, N. R., Bean, S. & Mullineaux, P. M. pGreen: a versatile and flexible
1012 binary Ti vector for Agrobacterium-mediated plant transformation. *Plant Mol Biol* **42**, 819–832 (2000).

1013 117. Xu, J. & Scheres, B. Dissection of Arabidopsis ADP-RIBOSYLATION FACTOR 1 Function in Epidermal
1014 Cell Polarity. *Plant Cell* **17**, 525–536 (2005).

1015 118. Chalkley, R. J. & Clauser, K. R. Modification site localization scoring: strategies and performance. *Mol Cell*
1016 *Proteom Mcp* **11**, 3–14 (2012).

1017 119. Eisen, M. B., Spellman, P. T., Brown, P. O. & Botstein, D. Cluster analysis and display of genome-wide
1018 expression patterns. *Proceedings of the National Academy of Sciences of the United States of America* **95**, 14863
1019 14868 (1998).

1020 120. Zulawski, M., Schulze, G., Braginets, R., Hartmann, S. & Schulze, W. X. The Arabidopsis Kinome: phylogeny
1021 and evolutionary insights into functional diversification. *Bmc Genomics* **15**, 548 (2014).

1022 121. Maere, S., Heymans, K. & Kuiper, M. BiNGO: a Cytoscape plugin to assess overrepresentation of Gene
1023 Ontology categories in Biological Networks. *Bioinformatics* **21**, 3448–3449 (2005).

1024 122. Komis, G., Takáč, T., Bekešová, S., Vadovič, P. & Samaj, J. Affinity-based SDS PAGE identification of
1025 phosphorylated Arabidopsis MAPKs and substrates by acrylamide pendant Phos-Tag™. *Methods Mol Biology*
1026 *Clifton N J* **1171**, 47–63 (2014).

1027

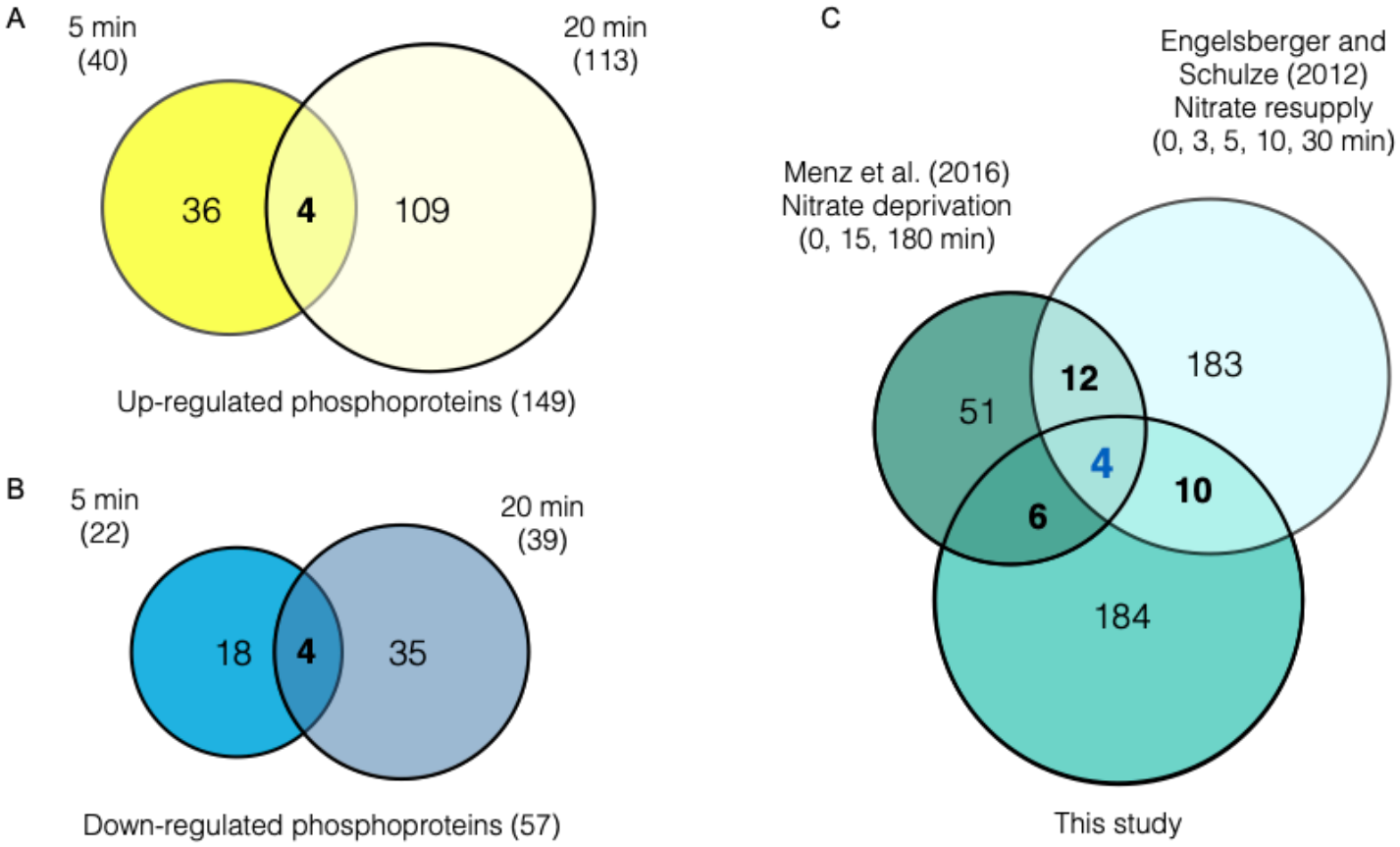

Figure 1

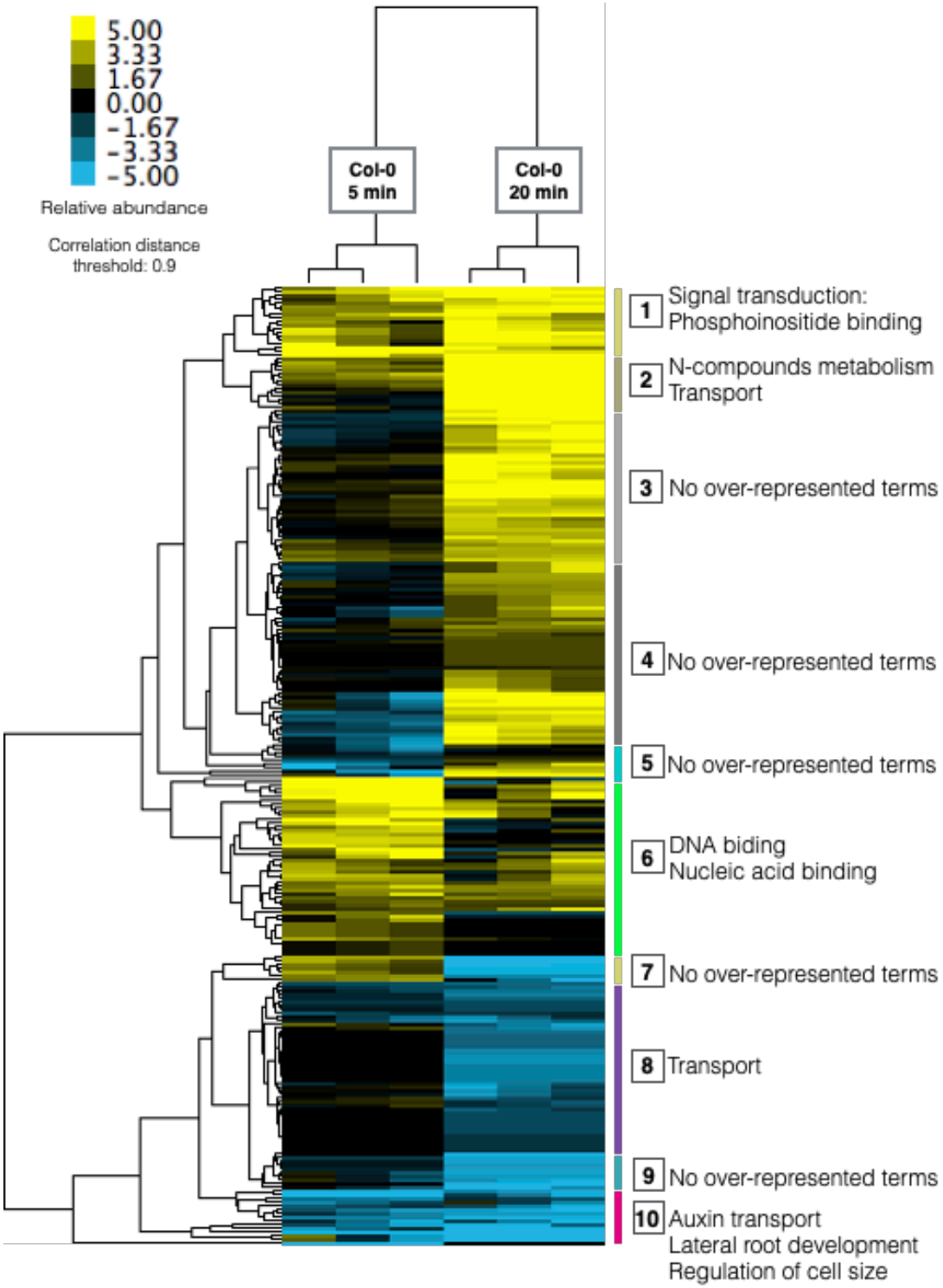

Figure 2

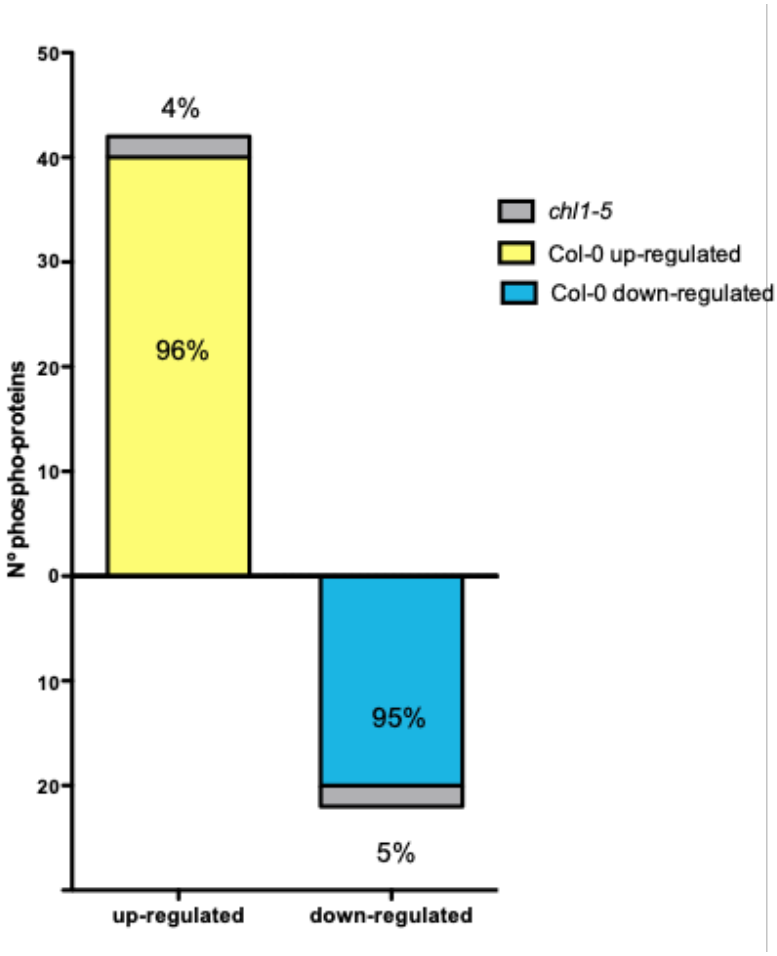

Figure 3

A

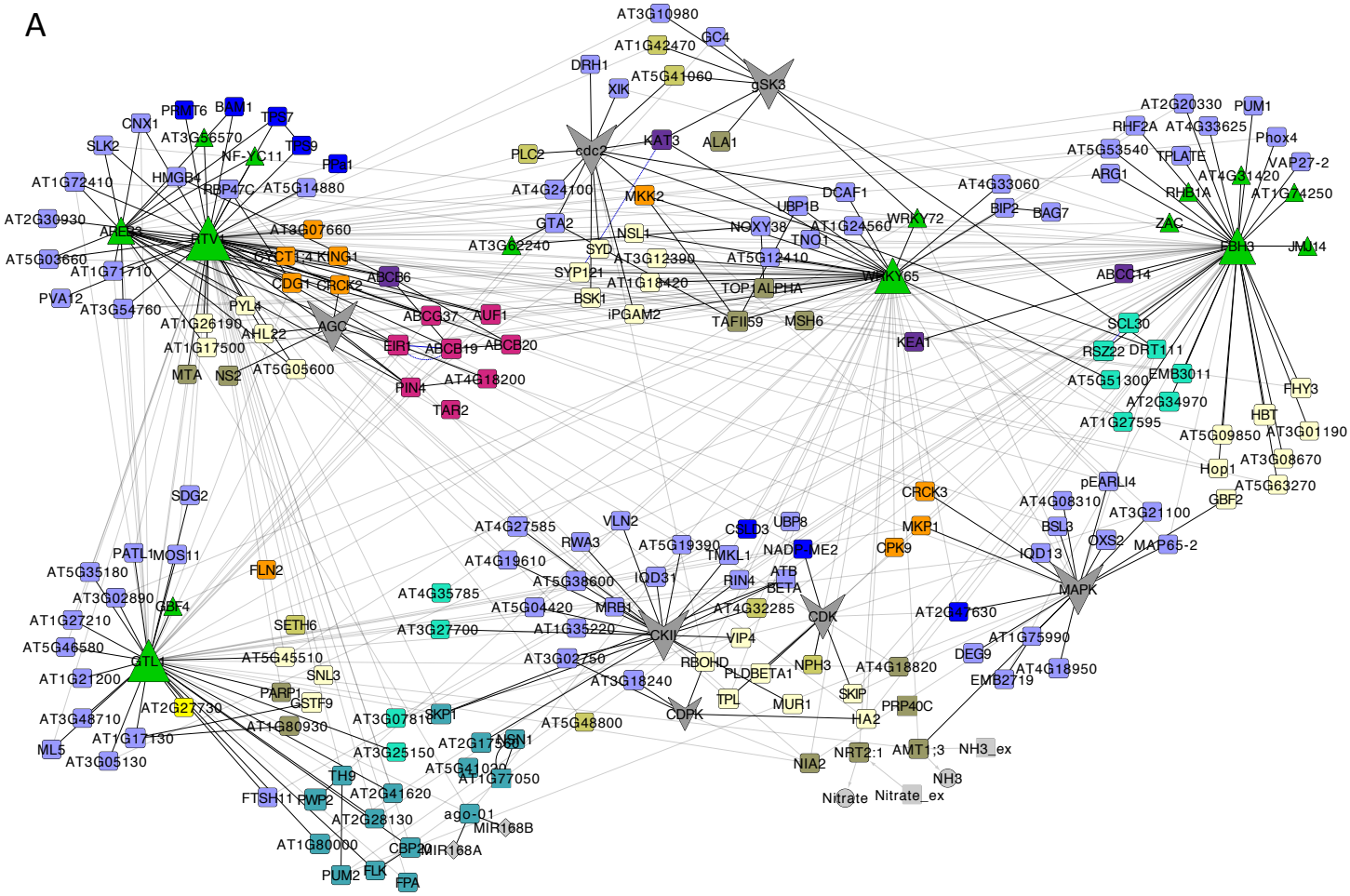

B

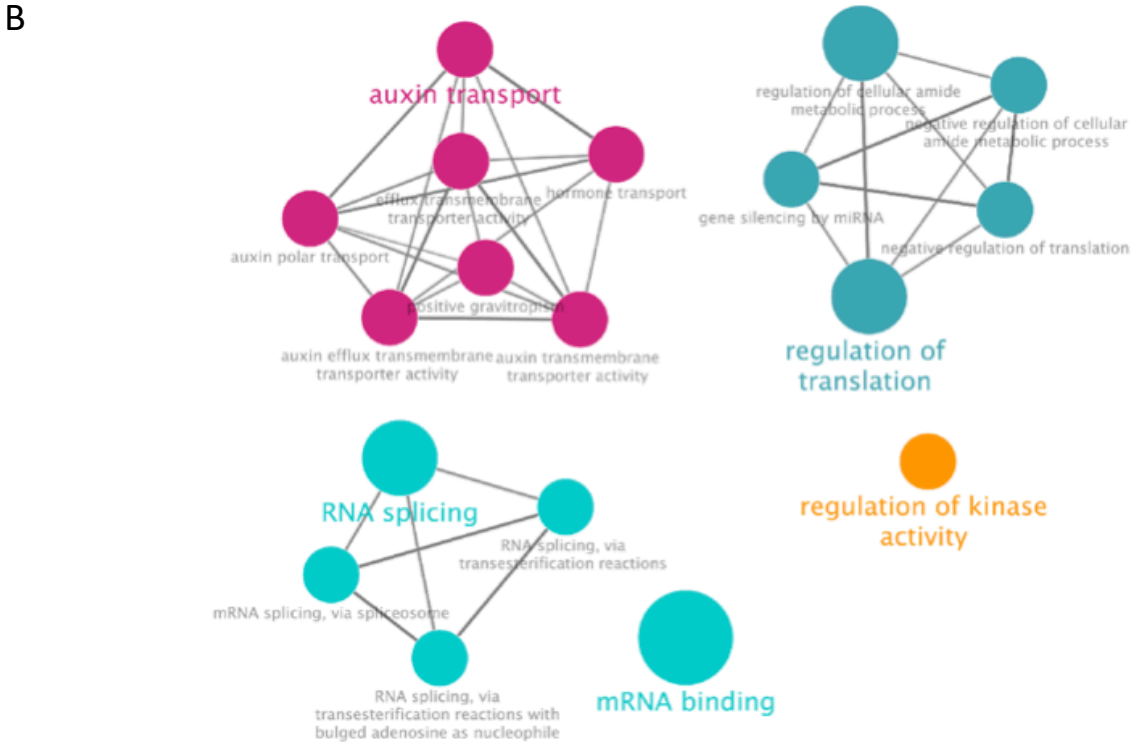

Figure 4

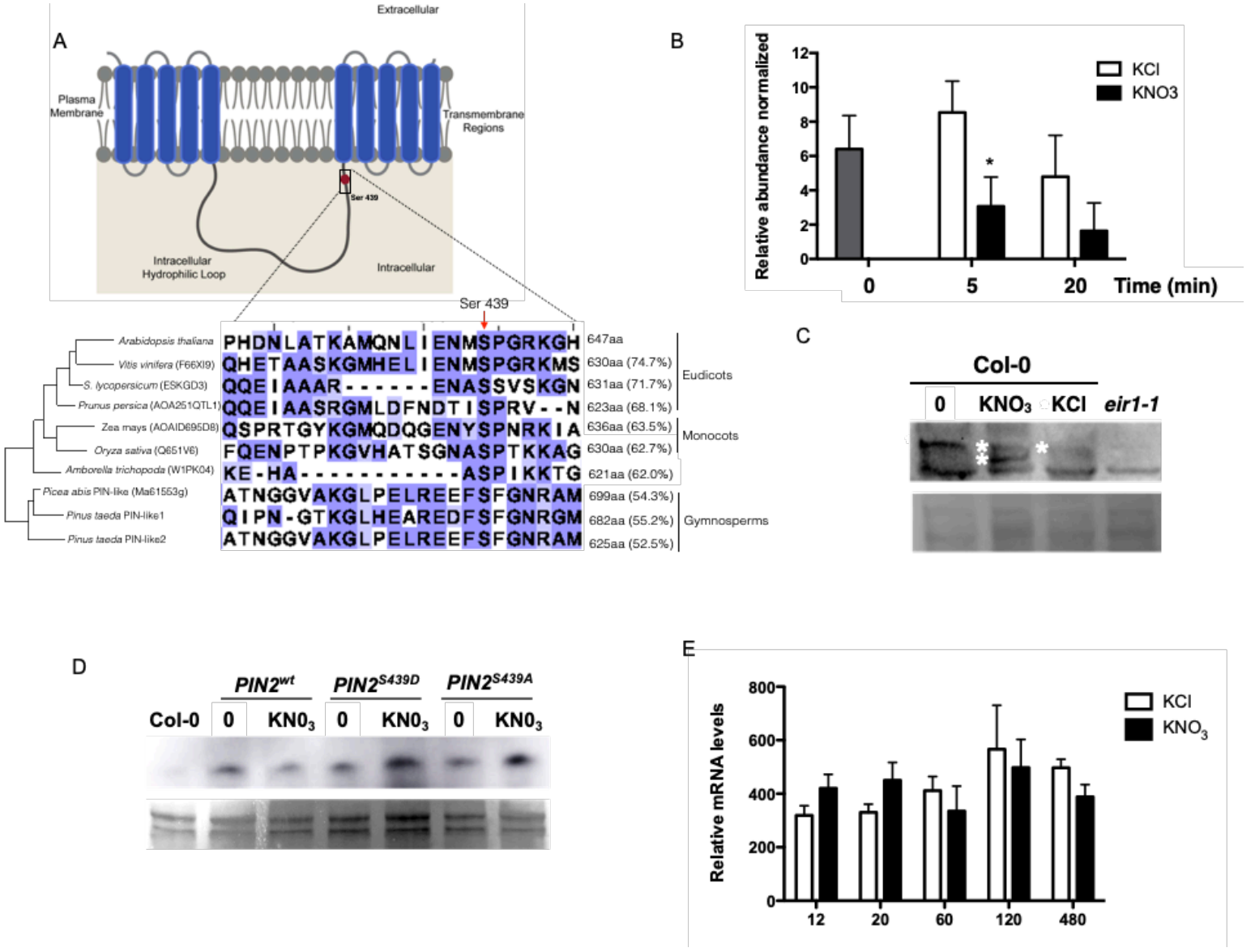

Figure 5

A

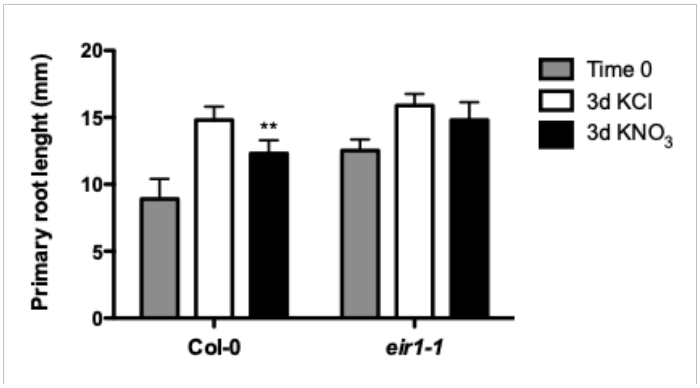

B

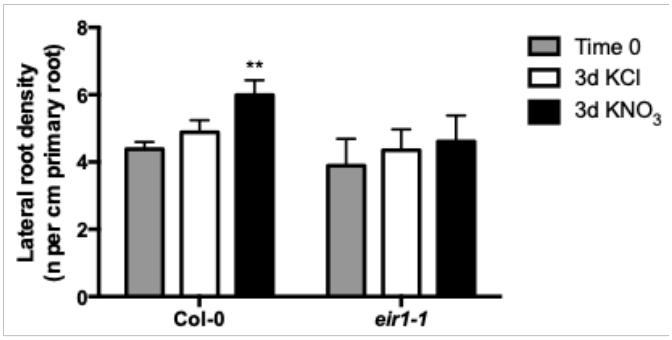

Figure 6

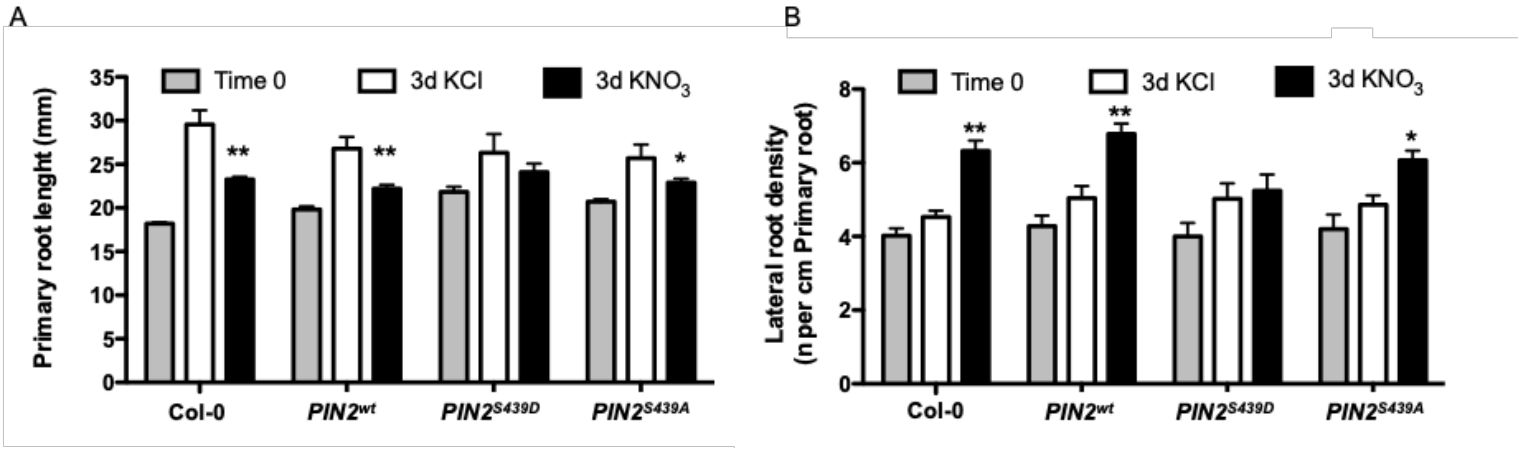

Figure 7

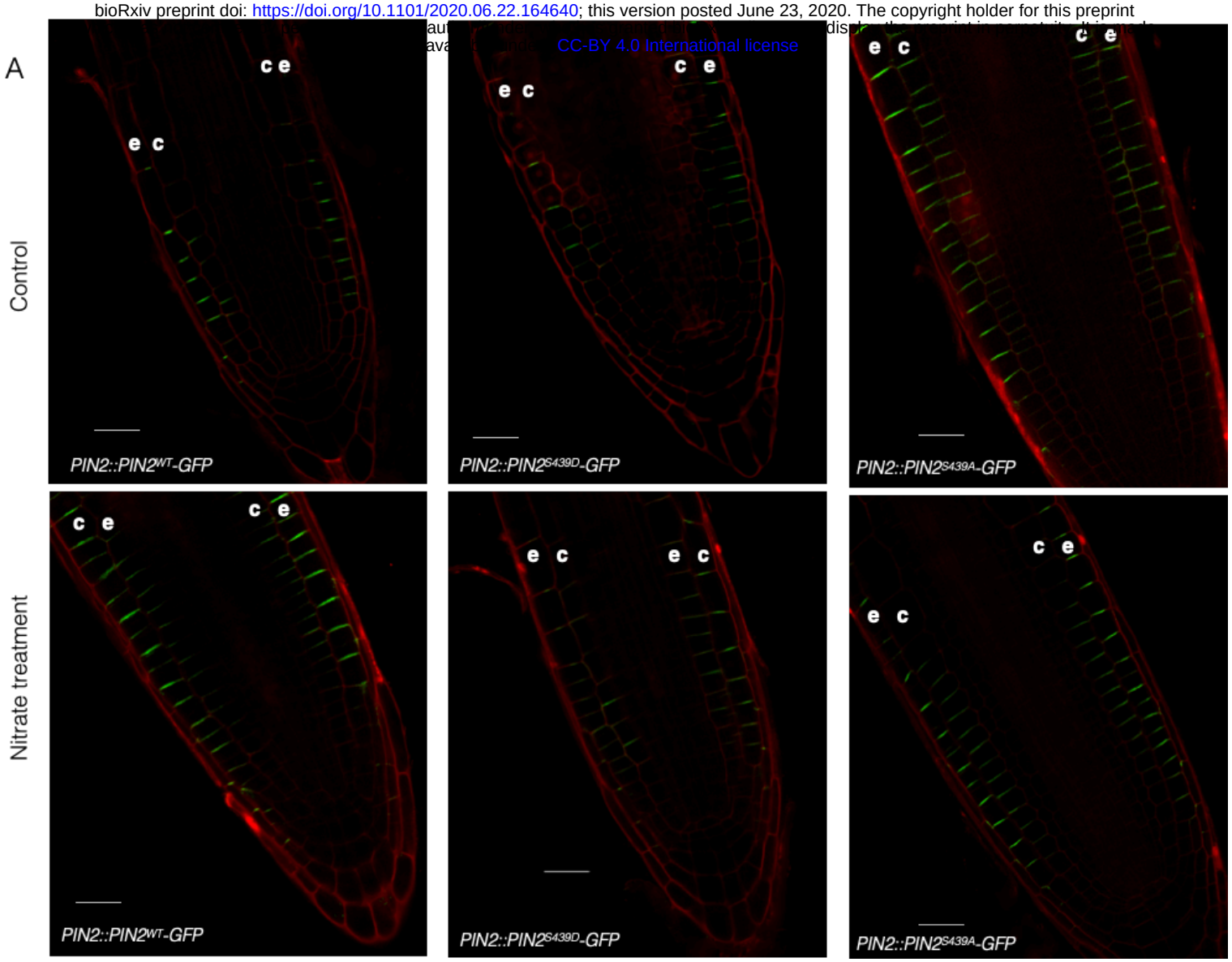

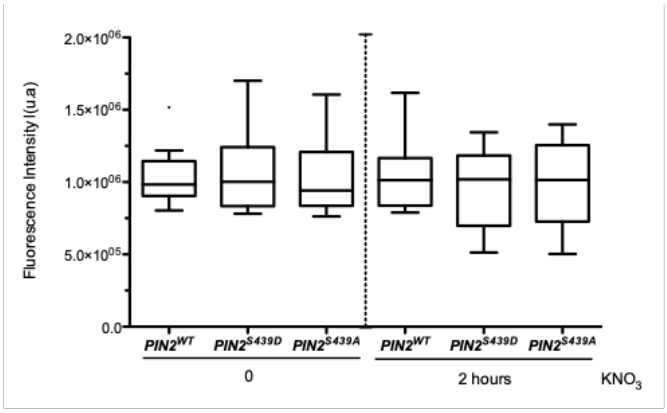

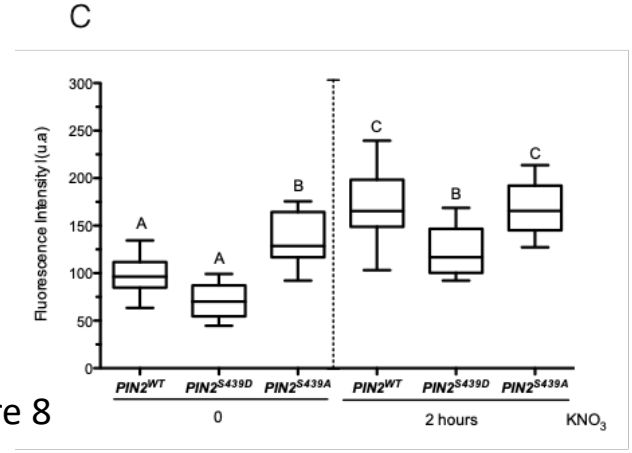

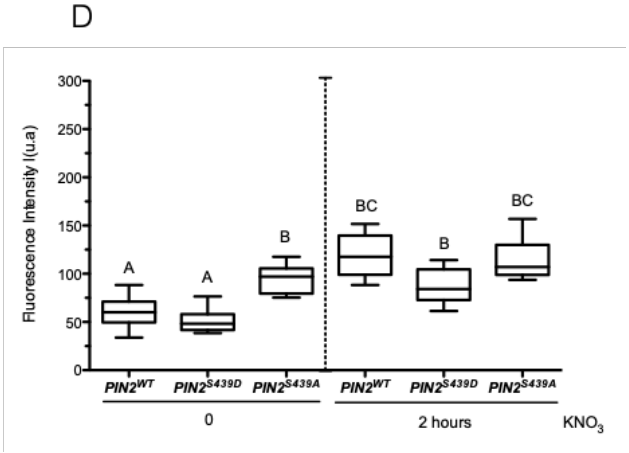

Figure 8

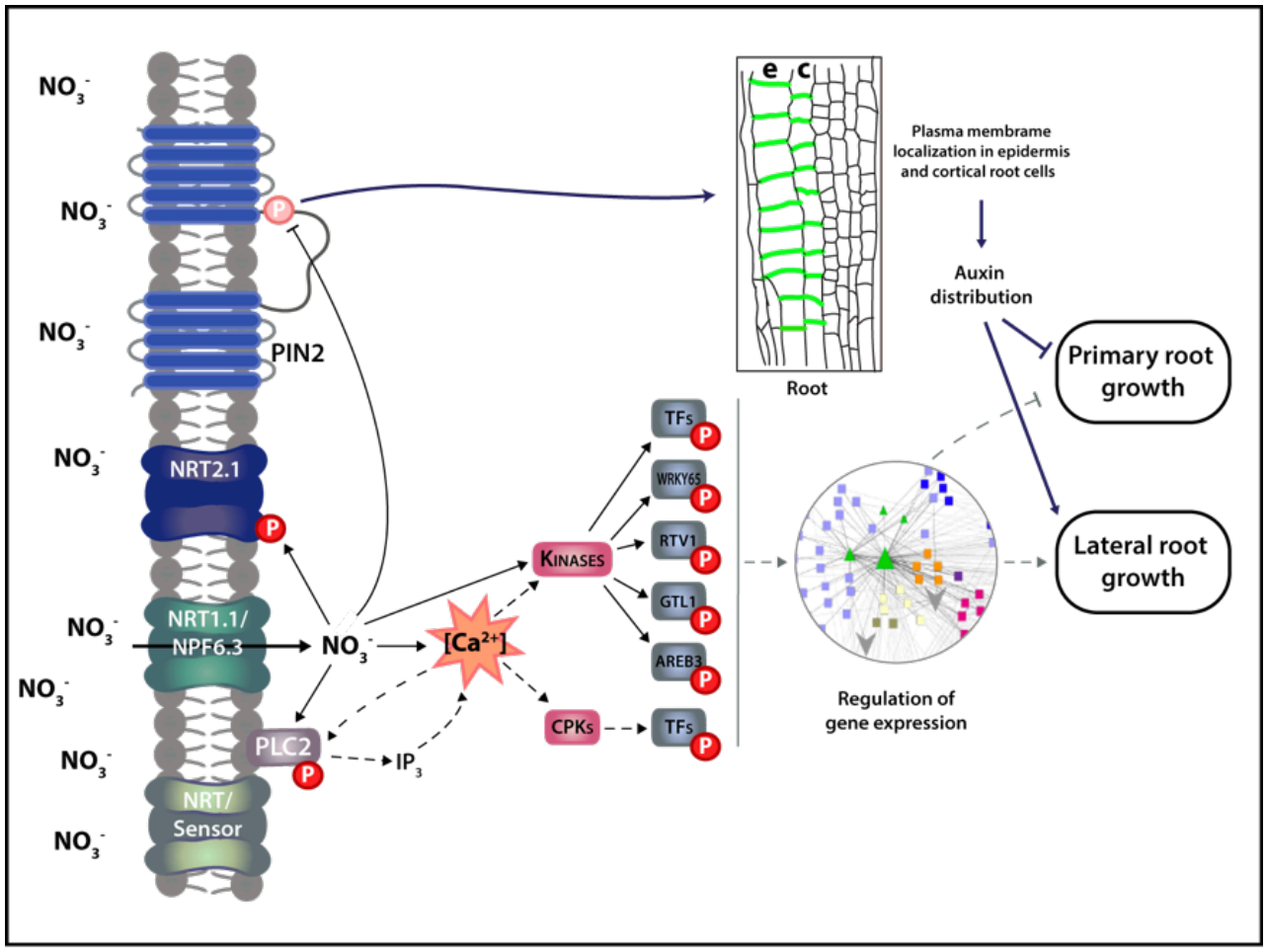

Figure 9

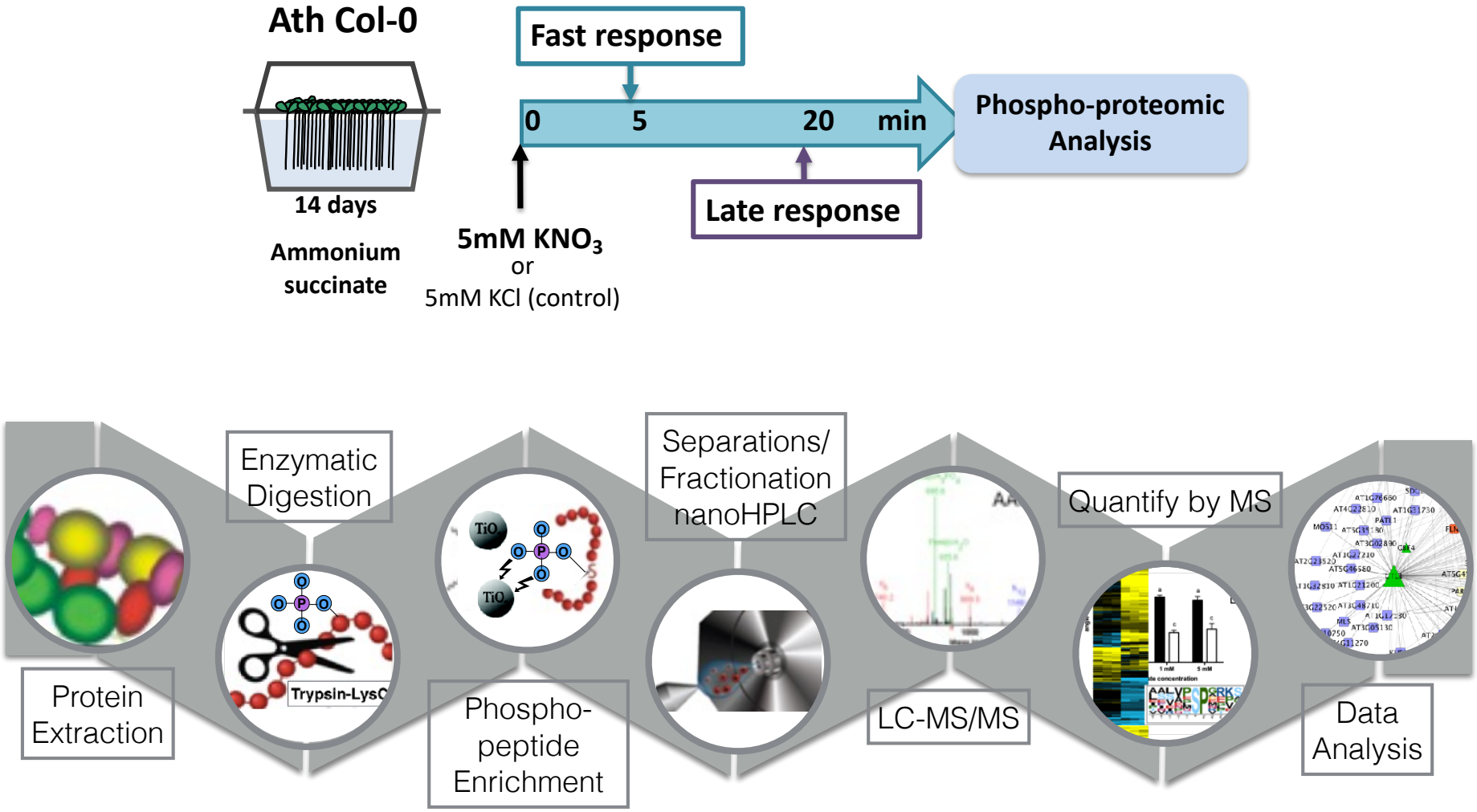
Ath Col-0
14 days
Ammonium succinate
Fast response
0
5
20
min
Late response
5mM KNO3
or
5mM KCl (control)
Phospho-proteomic Analysis
Protein Extraction
Enzymatic Digestion
Trypsin-LysC
Phospho-peptide Enrichment
TiO
Separations/ Fractionation nanoHPLC
LC-MS/MS
Quantify by MS
Data Analysis

Figure S1

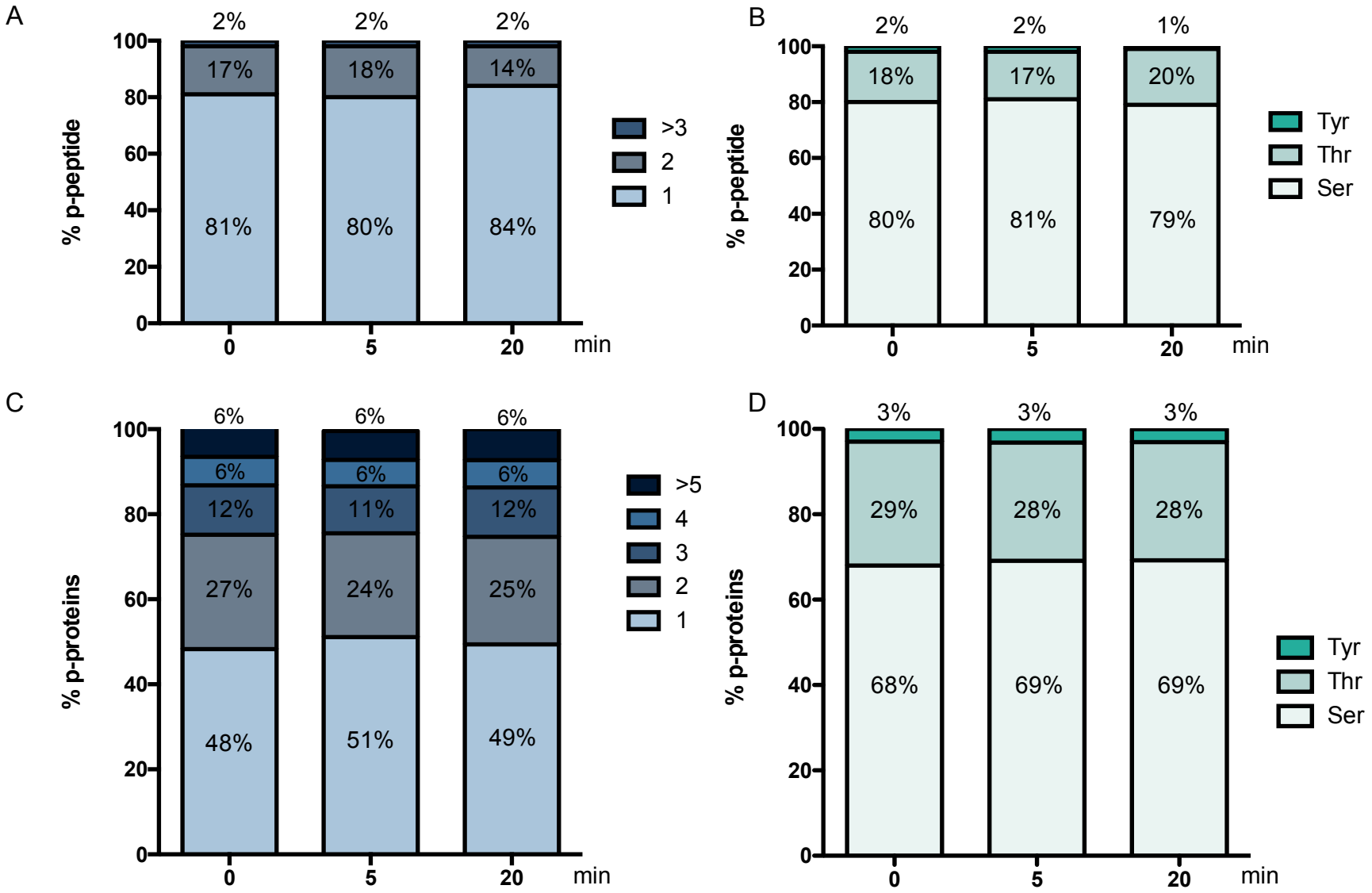
A
2%
2%
2%
17%
18%
14%
81%
80%
84%
100
80
60
40
20
0
% p-peptide
0
5
20
min
>3
2
1
B
2%
2%
1%
18%
17%
20%
80%
81%
79%
% p-peptide
Tyr
Thr
Ser
C
6%
6%
6%
6%
6%
6%
12%
11%
12%
27%
24%
25%
48%
51%
49%
% p-proteins
>5
4
3
2
1
D
3%
3%
3%
29%
28%
28%
68%
69%
69%
% p-proteins
Tyr
Thr
Ser

Figure S2.

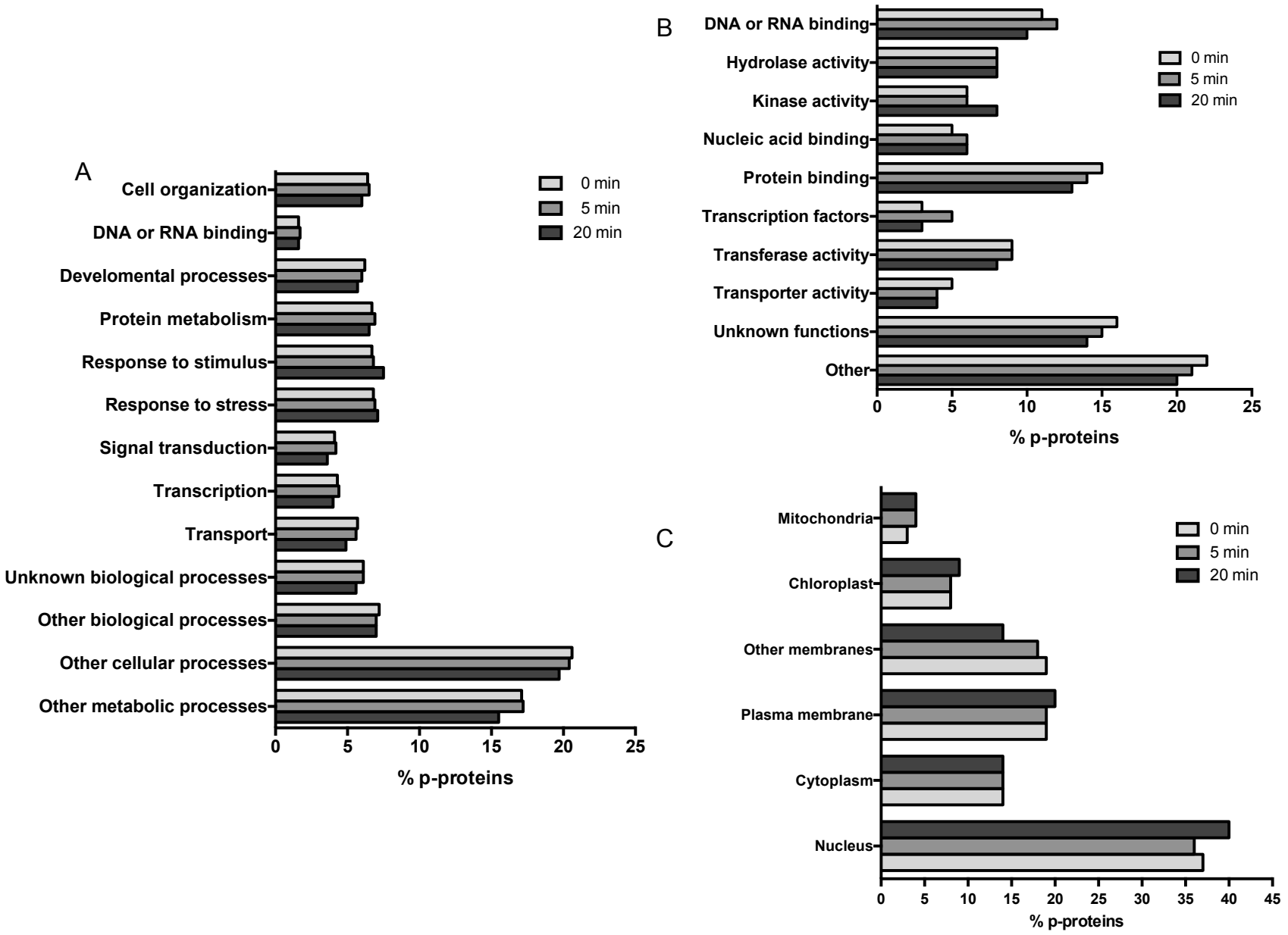
A
Cell organization
DNA or RNA binding
Develomental processes
Protein metabolism
Response to stimulus
Response to stress
Signal transduction
Transcription
Transport
Unknown biological processes
Other biological processes
Other cellular processes
Other metabolic processes
0 min
5 min
20 min
0
5
10
15
20
25
% p-proteins
B
DNA or RNA binding
Hydrolase activity
Kinase activity
Nucleic acid binding
Protein binding
Transcription factors
Transferase activity
Transporter activity
Unknown functions
Other
0 min
5 min
20 min
0
5
10
15
20
25
% p-proteins
C
Mitochondria
Chloroplast
Other membranes
Plasma membrane
Cytoplasm
Nucleus
0 min
5 min
20 min
0
5
10
15
20
25
30
35
40
45
% p-proteins

Figure S3.

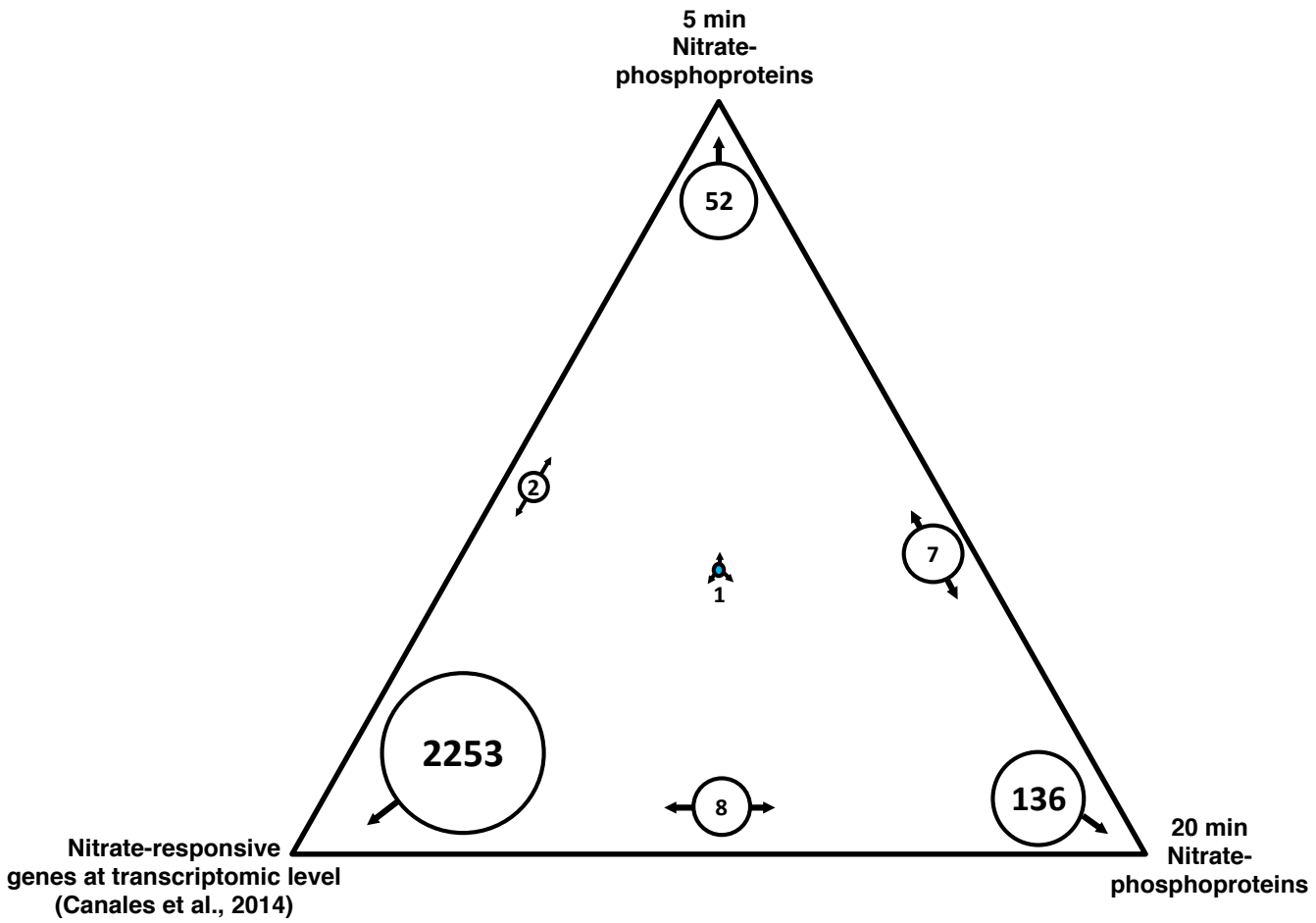
5 min
Nitrate-
phosphoproteins
52
2
1
7
2253
8
136
Nitrate-responsive
genes at transcriptomic level
(Canales et al., 2014)
20 min
Nitrate-
phosphoproteins

Figure S4.

A

B

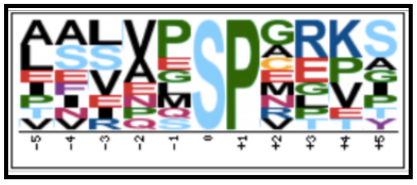

C

D

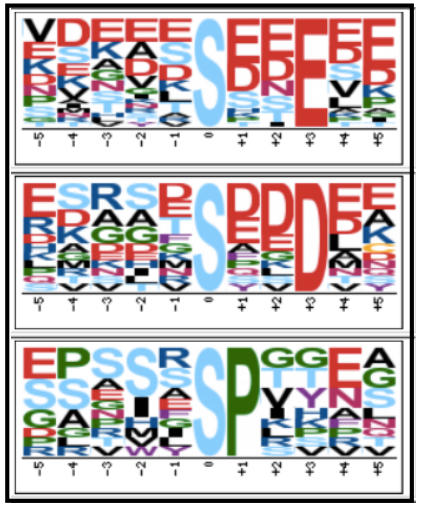

Figure S5

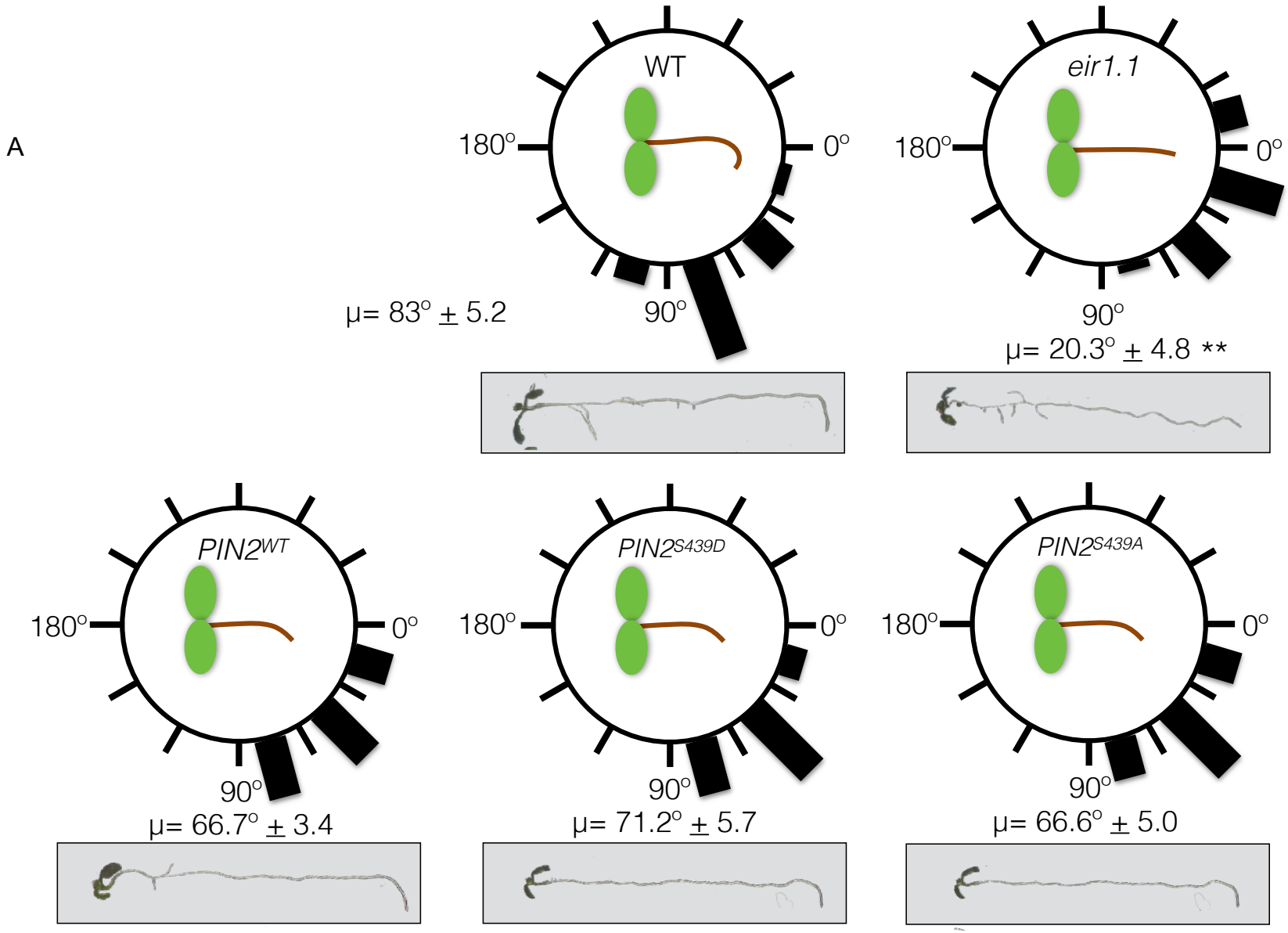
A
WT
180°
0°
90°
μ= 83° ± 5.2
eir1.1
180°
0°
90°
μ= 20.3° ± 4.8 **
PIN2WT
180°
0°
90°
μ= 66.7° ± 3.4
PIN2S439D
180°
0°
90°
μ= 71.2° ± 5.7
PIN2S439A
180°
0°
90°
μ= 66.6° ± 5.0

Figure S6.

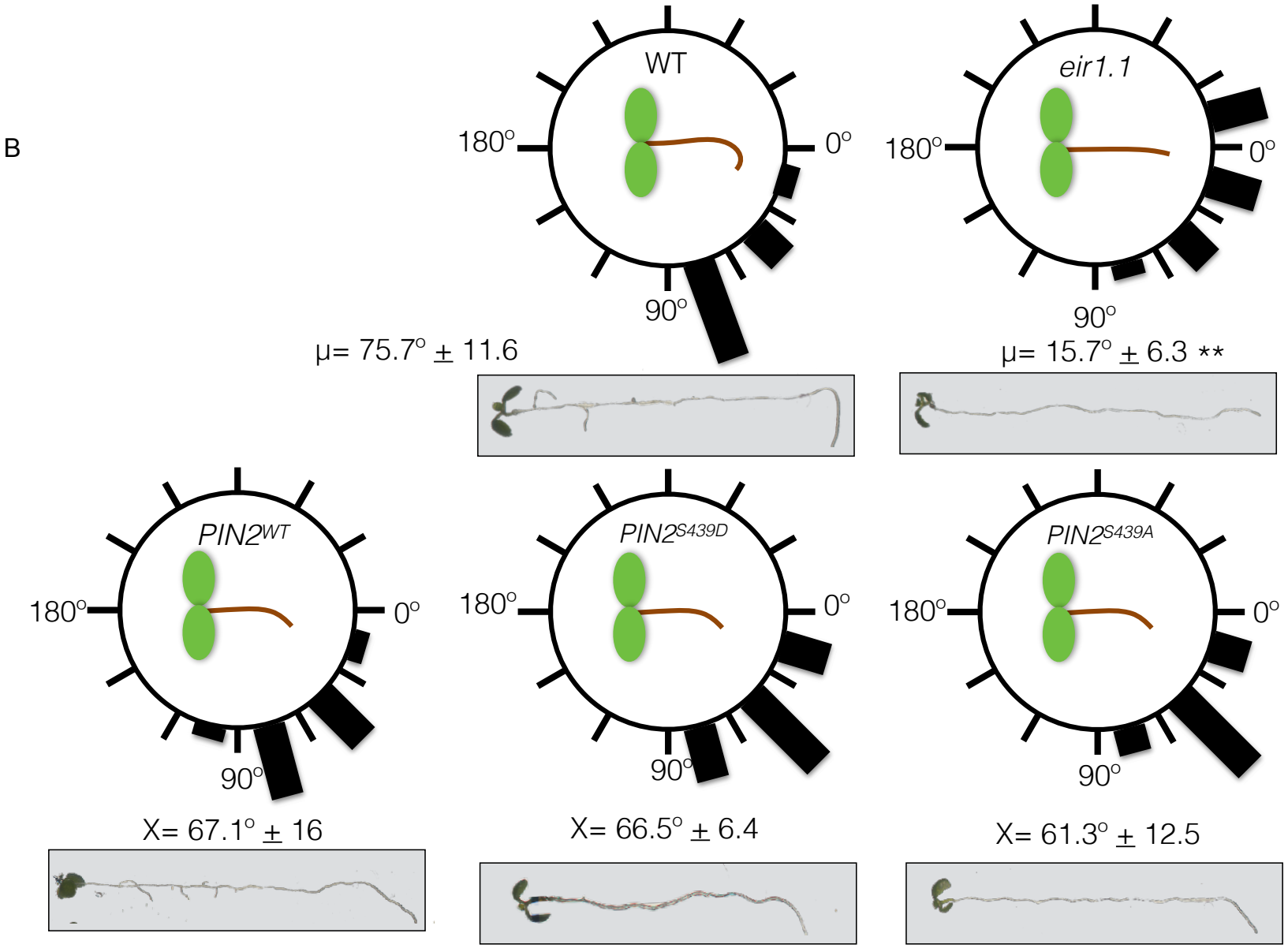
B
WT
180°
0°
90°
μ= 75.7° ± 11.6
eir1.1
180°
0°
90°
μ= 15.7° ± 6.3 **
PIN2WT
180°
0°
90°
X= 67.1° ± 16
PIN2S439D
180°
0°
90°
X= 66.5° ± 6.4
PIN2S439A
180°
0°
90°
X= 61.3° ± 12.5

Figure S6.